

UNIVERSITY OF OKLAHOMA
GRADUATE COLLEGE

EVALUATION OF PHOSPHATE RECOVERY AND RELEASE PERFORMANCE OF
CALCIUM SILICATE HYDRATE MADE FROM RICE HUSK

A THESIS
SUBMITTED TO THE GRADUATE FACULTY
in partial fulfillment of the requirements for the
Degree of
MASTER OF SCIENCE IN ENVIRONMENTAL ENGINEERING

By
NUSRAT SHARMIN
Norman, Oklahoma
2020

EVALUATION OF PHOSPHATE RECOVERY AND RELEASE PERFORMANCE OF
CALCIUM SILICATE HYDRATE MADE FROM RICE HUSK

A THESIS APPROVED FOR THE
SCHOOL OF CIVIL ENGINEERING AND ENVIRONMENTAL SCIENCE

BY THE COMMITTEE CONSISTING OF

Dr. Elizabeth Butler, Chair

Dr. David Sabatini, Co-chair

Dr. Robert Nairn

Acknowledgements

I start by expressing my gratitude to God Almighty for giving the strength and patience to complete this research. I would like to thank my advisor Dr. Elizabeth Butler for her continuous support and guidance throughout my whole master's journey. She was patient with me whenever I made mistakes and motivated me to excel in my work. I would also like to thank my co-advisor Dr. David Sabatini for sharing his insightful comments and suggestions throughout this endeavor. Many thanks to Dr. Robert Nairn for taking the time to serve as my committee member and for his invaluable input in refining this thesis.

I would like to acknowledge USDA National Institute of Food and Agriculture for funding this project through Agriculture and Food Research Initiative (AFRI) Grant. I express my gratitude to Anna McClung and Laduska Sells of USDA Agricultural Research Service, Dale Bumpers National Rice Research Center, Stuttgart, Arkansas for providing the rice straw as research material. Special thanks to Dr. Preston Larson and Dr. Andrew S. Madden for their help with SEM and XRD analysis. I would also like to thank my current and previous lab mates: Parichat Phaodee, Anisha Nijhawan, Phillip Deal, Ian Thom, and Yifan Ding for their words of encouragement and friendship. I am especially grateful to Yifan Ding for doing the phosphorus release experiments during the corona virus pandemic situation.

Lastly, I want to thank my family and friends in Bangladesh for their unconditional love and prayers. I express my deepest love and gratitude to my husband Mushfiqur Rahman, thank you for believing me more than I believed in myself.

Table of Contents

Acknowledgements.....	iv
Table of Contents.....	v
List of Tables	vii
List of Figures.....	viii
Abstract.....	xi
Chapter 1: Introduction.....	1
1.1 Methods for phosphorus removal and recovery from wastewater	2
1.2 Phosphate recovery by calcium silicate hydrate made from waste materials.....	3
1.3 Mechanism of phosphate uptake by calcium silicate hydrate	4
1.4 Phosphorus release from used calcium silicate hydrate	6
1.5 Hypotheses and objectives of this research	7
1.6 Thesis overview	7
Chapter 2: Materials and Methods.....	9
2.1 Preparation of ash from rice husk and rice straw	9
2.2 Preparation of calcium silicate hydrate: Method 1	9
2.3 Preparation of calcium silicate hydrate: Method 2	10
2.4 Material characterization	11
2.5 Phosphorus uptake experiments	11
2.6 Phosphorus release experiments.....	14
Chapter 3: Results and Discussion.....	17
3.1 Chemical composition of ash from rice husk and rice straw.....	17

3.2	Characterization of the synthesized calcium silicate hydrate	18
3.3	Phosphorus uptake by calcium silicate hydrate	21
3.4	Phosphorus release by spent calcium silicate hydrate	29
3.5	Cost comparison of calcium silicate hydrate with commercially available fertilizer.	31
Chapter 4: Conclusions and Recommendations		33
4.1	Conclusions	33
4.2	Recommendations for practice	34
4.3	Recommendations for future research.....	35
Appendix A: Preparation of calibration standards.....		36
Appendix B: SEM images of rice husk ash, rice straw ash and calcium silicate hydrate (calcite-tobermorite mixture).....		37
Appendix C: Preliminary experiments done with calcite-tobermorite mixture.....		39
Appendix D: Cost analysis.....		43
D.1	Production cost of one ton calcium silicate hydrate	43
D.2	Cost comparison of one ton phosphorus from calcium silicate hydrate and DAP fertilizer..	46
D.3	Cost improvement by using lime to synthesize calcium silicate hydrate	47
References.....		50

List of Tables

Table 1 Composition of extractants used in Mehlich 3, Bray P1 and Olsen soil phosphorus tests.	15
Table 2 Composition of ash from rice husk and rice straw based on EDS analysis	18
Table D.1 Summary of costs for production of one ton calcium silicate hydrate.....	45
Table D.2 Cost comparison of the prices for one ton phosphorus from calcium silicate hydrate and DAP fertilizer.....	47
Table D.3 Revised cost for production of one ton calcium silicate hydrate synthesized from lime instead of NaOH and $\text{Ca}(\text{NO}_3)_2 \cdot 4\text{H}_2\text{O}$	48
Table D.4 Revised comparison of the prices for one ton phosphorus from calcium silicate hydrate (synthesized from lime) and from DAP fertilizer.	49

List of Figures

- Fig. 1.** XRD patterns of (a) calcite-tobermorite mixture synthesized with system open to atmosphere, (b) rice husk ash, (c) opal and (d) calcium silicate hydrate synthesized with system closed to atmosphere. Symbols: calcite (●), tobermorite (■), silicon oxide (SiO₂ ITQ-07) (▲) and calcium silicate hydrate-CSH (◆). The XRD patterns of opal, calcite, tobermorite and silicon oxide (SiO₂ ITQ-07) was obtained from the Powder Diffraction File database of International Center for Diffraction Data (ICDD). The peak location of calcium silicate hydrate was taken from Houston et al. (2009)..... 19
- Fig. 2.** Phosphate uptake by calcite-tobermorite mixture (synthesized open to atmosphere) and calcium silicate hydrate (synthesized closed to atmosphere). Material dosage and equilibrium pH were 2 g/L and 9, respectively. The inset panel indicates phosphate uptake at lower equilibrium phosphate concentrations. The error bars represent the standard deviations of the means associated with Q_e and C_e calculated from duplicate measurements. 20
- Fig. 3.** Phosphate uptake by calcium silicate hydrate in deionized water with a dosage of 2 g/L and 3 g/L. The pH of the solutions was adjusted to 9. The error bars represent the standard deviations of the means associated with Q_e and C_e calculated from duplicate measurements. Large error bars for some data points could be due to the small sample size of 2 and/or the inhomogeneity of calcium silicate hydrate..... 21
- Fig. 4.** Phosphate uptake by calcium silicate hydrate at pH 8 and 9 with a dosage of 3 g/L. The inset panel indicates phosphate uptake at lower equilibrium phosphate concentrations. The error bars represent the standard deviations of the means associated with Q_e and C_e calculated from duplicate measurements. Large error bars for some data points could be due to the small sample size of 2 and/or the inhomogeneity of calcium silicate hydrate..... 22

Fig. 5. Solubilities of calcium phosphate minerals calculated separately for each solid, with MINEQL+ version 5.0. Concentration of total calcium was assumed as 0.001 M and phosphate solubility was controlled by the mineral/water equilibrium. Formation constants of all minerals were from MINEQL+ database. 24

Fig. 6. Phosphate uptake by calcium silicate hydrate in model dairy wastewater at pH 8, 9 and 10. Total alkalinity of the wastewater was calculated to be 4723, 5000 and 6120 mg/L as CaCO₃ at pH 8, 9 and 10, respectively (by applying ionic strength corrections in MINEQL+ version 5.0). The error bars represent the standard deviations of the means associated with Q_e and C_e calculated from duplicate measurements. 26

Fig. 7. XRD patterns of precipitated solids collected from (a) model dairy wastewater with no phosphate, (b) model dairy wastewater with 68.5 mg P/L (c) deionized water with no phosphate (d) deionized water with 68.5 mg P/L and (e) XRD pattern of calcite obtained from the Powder Diffraction File database of International Center for Diffraction Data (ICDD). The arrows indicate unidentified peaks. All solutions mentioned above were adjusted to pH 9. 27

Fig. 8. Phosphate uptake by calcium silicate hydrate in model wastewaters containing total alkalinity ranging from 0-5000 mg/L as CaCO₃ at pH 9. Inset panel indicates phosphate uptake in wastewaters containing 0-300 mg/L as CaCO₃ at pH 9. The error bars represent the standard deviations of the means associated with Q_e and C_e calculated from duplicate measurements. Error bars are not shown for the data in the inset so the trends could be illustrated more clearly. 29

Fig. 9. Phosphorus release by precipitated solids collected from phosphate solutions of deionized water and model dairy wastewater (initial phosphate concentration 68.5 mg P/L). Solid to extractant ratio was 1:800 (w/v). The relative standard deviation ranged from 1-4% for measurements made in standard solutions of NaH₂PO₄. 30

Fig. A.1 Example of a calibration curve.....	36
Fig. B.1. SEM image of rice husk ash.	37
Fig. B.2. SEM image of rice straw ash.	37
Fig. B.3. SEM image of calcite-tobermorite mixture made from rice husk ash (synthesized with system open to atmosphere).....	38
Fig. B.4. SEM image of calcium silicate hydrate made from rice straw ash (made with system open to atmosphere).....	38
Fig. C.1. Phosphate uptake by calcite-tobermorite mixture at pH 7, 8, 9 and 10 with initial phosphate concentrations of 0.69-68.5 mg P/L and dosage 2 g/L. The inset panel indicates phosphate uptake at lower equilibrium phosphate concentrations. The error bars represent the standard deviations of the means associated with Q_e and C_e calculated from duplicate measurements.....	40
Fig. C.2. Concentrations of Ca^{2+} measured experimentally and theoretically from the solubility products of: brushite ($CaHPO_4 \cdot 2H_2O$), monetite ($CaHPO_4$), octacalcium phosphate ($Ca_4H(PO_4)_3 \cdot 3H_2O$), β - tricalcium phosphate ($\beta-Ca_3(PO_4)_2$) and hydroxyapatite ($Ca_5(PO_4)_3OH$) in phosphate solutions of deionized water at pH 10. Symbols for $\beta-Ca_3(PO_4)_2$ are below the symbols of $Ca_4H(PO_4)_3 \cdot 3H_2O$	42

Abstract

In this study, calcium silicate hydrate was synthesized using silica-rich rice husk for recovering phosphorus from wastewater and reusing it as fertilizer under simulated soil conditions. By controlling pH and inhibiting calcite formation during synthesis, a non-crystalline form of calcium silicate hydrate was produced which showed significantly higher phosphate uptake capacity. The driving force for phosphate uptake by calcium silicate hydrate was identified as the presence of sufficient amount of Ca^{2+} and PO_4^{3-} ions to cause supersaturation and precipitation of calcium phosphate. Calcium silicate hydrate was able to uptake 99% of the total phosphate from solutions of deionized water (for initial concentration of 68.5 mg P/L, equilibrium pH 9). The removal capacity of calcium silicate hydrate was substantially decreased in a high alkalinity system (4936 mg/L as CaCO_3), modeling the concentrations of anaerobic treatment effluent of dairy manure, due to the formation of calcite instead of calcium phosphate. By gradually decreasing the alkalinity, a proportionate increase in phosphate uptake was observed, and model wastewaters with alkalinity levels of 100, 200 and 300 mg/L as CaCO_3 showed similar phosphate uptake ($\geq 99\%$) as deionized water (without any alkalinity). Phosphorus was extracted from spent calcium silicate hydrate by modified methods of soil phosphorus tests, i.e., Mehlich 3, Bray P1 and Olsen simulating conditions of neutral, acidic, and alkaline soil, respectively. The precipitated solids in deionized water released a relatively lower amount of phosphorus in Mehlich 3 extractant, which only measures the adsorbed form of phosphorus. This suggested that most of the phosphorus in deionized water solutions was removed by precipitation of a phosphate mineral and not by adsorption. Olsen test performed poorly to estimate the released phosphorus from solids collected from the high alkalinity wastewater, because of the increased concentration of HCO_3^- prevailing in the system.

Chapter 1: Introduction

Phosphorus is an essential nutrient for food production and plays a vital role in cell development in all living organisms. Phosphorus is primarily mined as phosphate rock with about 85% of mined phosphorus being used in fertilizer production; almost half of it is eventually lost to the environment through agricultural runoff, soil erosion and animal wastes (Rittman et al., 2011). Although a recent report showed a four-fold increase in the global reserve of phosphate rock (IFDC 2010), this increase was linked to inconsistent quantification of reserves and resources and was not the result of new discovery of phosphate rock deposits (Edixhoven et al., 2014). Scholars have debated about how much of this reported reserve is economically and environmentally feasible to extract and whether it would be sufficient to meet future agricultural needs (Cordell et al, 2009; Schröder et al, 2010). In addition, phosphorus-rich wastewaters released to surface water leads to the acceleration of algal blooms and eutrophication, harming both human and aquatic life (Correll, 1998). Therefore, it is necessary to close the phosphorus cycle by recovering it from waste sources and reusing it as fertilizer.

Effluents from the anaerobic treatment of dairy and swine manure contain significant amount of phosphorus (69-150 mg/L of $\text{PO}_4\text{-P}$) (Sanchez et al., 2000; Vanotti et al., 2003; Huchzermeier and Tao, 2012), but direct application of these wastewaters to crop lands can compromise food safety due to the potential for transmitting pathogens (Resende et al., 2014; Alfa et al., 2014). To be used as an effective fertilizer, phosphorus removed from wastewater needs to be released in soil efficiently without raising any aesthetic or regulatory concerns. Furthermore, the process of recovering and reusing phosphorus should ensure utilization of low-cost and non-toxic raw materials to offset the higher cost and environmental impacts associated with phosphate rock mining.

1.1 Methods for phosphorus removal and recovery from wastewater

The most common method of removing phosphorus from wastewater is by chemical precipitation with metal salts, e.g., precipitation of calcium, magnesium, aluminum and iron phosphates (Aguilar et al., 2002; Chuang et al., 2006; Perera et al., 2007; Georgantas and Grigoropoulou, 2007; Gungor and Karthikeyan, 2008; Banu et al., 2008; Jordaan et al., 2010; Caravelli et al., 2010). Although low levels of aqueous phosphorus (1-2 mg P/L) can be achieved in the effluent by aluminum and iron phosphate precipitation (Desmidt et al., 2015), it is difficult to recover phosphorus from these minerals or use them as fertilizers due to their low solubility under typical soil conditions (Rittman et al., 2011) and their toxicity towards many plants when dissolved in acidic soil solutions (Sahrawat, 2004; Panda et al., 2009). Precipitation by magnesium and calcium salts is a preferred method for phosphate recovery and reuse as the precipitated solids exhibit qualities similar to those of standard fertilizers such as slow release of bioavailable phosphorus and high solubility in soil solution (Johnston and Richards., 2003; Plaza et al., 2007; Cabeza et al., 2011). Struvite (MgNH_4PO_4) precipitation is a popular method to remove both nitrogen and phosphorus from anaerobic digester effluents (Burns et al., 2002; Rittman et al., 2011; Zhou et al., 2014, Kumar and Pal, 2015; Shu et al., 2019), but often additional treatment steps like seeding, supplementing with magnesium/ammonium salts and removal of calcium ion are required for successful precipitation of pure product (Huchzermeier and Tao, 2012), all of which ultimately increase overall process cost.

Calcium enriched minerals have been used as a source of Ca^{2+} ions to precipitate calcium phosphate from phosphorus-rich wastewaters (Giesen, 1999; Oladoja et al., 2013; Guan et al., 2014). Examples of calcium compounds used so far include calcite (CaCO_3), dolomite ($\text{CaMg}(\text{CO}_3)_2$), and synthesized calcium silicate hydrates (xonotlite ($\text{Ca}_6\text{Si}_6\text{O}_{17}(\text{OH})_2$),

tobermorite ($5\text{CaO}\cdot 6\text{SiO}_2\cdot 5\text{H}_2\text{O}$), amorphous calcium silicate hydrate) which are summarized in the review article of Peng et al. (2018).

1.2 Phosphate recovery by calcium silicate hydrate made from waste materials

Calcium silicate hydrate is preferred over other calcium minerals (e.g., calcium carbonate) to remove phosphorus from wastewater because it can act as a calcium ion donor while also raising the solution pH to 8-12, which together are favorable for precipitation of certain calcium phosphates (e.g. hydroxyapatite) (Okano et al., 2015; Jiang et al., 2017; Zhang et al., 2019). Also, the phosphorus laden calcium silicate hydrates can be directly recovered and reused as fertilizers (Okano et al., 2016). For low cost production of calcium silicate hydrates, a wide variety of calcium or silica rich wastes, such as crushed concrete, carbide residue, oyster shell and waste glass, have been utilized and the resultant materials were able to adsorb/precipitate phosphorus (Chen et al., 2013; Kuwahara et al., 2013; Guan et al., 2013; Jiang et al., 2017; Fang et al., 2018, Okano et al., 2015). One silica-rich waste source has not yet been utilized to synthesize calcium silicate hydrate for phosphate uptake – agricultural waste materials. Many agricultural wastes are rich in silica, such as rice husk/straw (Balakrishnan et al. 2013), wheat hull (Tezioglu and Yucel, 2012), sugarcane (Vaibhav et al., 2015) and bamboo. Rice husk and straw are some of the most common agricultural by-products with worldwide annual productions of 120 million tons (Kumar et al., 2012) and 731 million tons (Karimi et al, 2006), respectively. Disposal of this enormous amount of waste is a problem as it is often burned in open fields causing smoke and breathable dust containing crystalline silica, that leads to diseases related to lungs and eyes (El Damatty and Hussain, 2009). Utilization of this non-toxic biowaste to produce a wastewater treatment material would not only contribute to environmental sustainability, but also to economic sustainability by producing high value fertilizer from a low-cost waste material. One possible drawback of using

rice residues in water treatment is the risk of arsenic contamination as it can accumulate in different parts of the rice plants such as root, straw, husk, and grain (Abedin et al., 2002). The severity of this bioaccumulation depends on the arsenic content of the paddy soil and irrigation water as well as on the nature of rice species (Islam et al., 2016). It is therefore necessary to examine the arsenic content of rice husk/straw samples before applying it in water treatment.

1.3 Mechanism of phosphate uptake by calcium silicate hydrate

The term ‘calcium silicate hydrate’ is used to denote a family of solid phases in the CaO-SiO₂-H₂O regime with compositions ranging from Ca₅H₂Si₆O₁₈.8H₂O to Ca₉H₂Si₆O₁₈(OH)₈.6H₂O (Nonat, 2004). In solution, the Ca-OH groups in calcium silicate hydrate release sufficient Ca²⁺ to create supersaturation of calcium phosphate in phosphorus rich wastewaters (Fang et al., 2018). Further, release of OH⁻ ions maintain the solution pH between 8-12, which is the range of minimum solubility for calcium phosphate minerals like hydroxyapatite and tricalcium phosphate (Chow, 1991). Most researchers agree that precipitation of calcium phosphate minerals is the main mechanism behind phosphate uptake by calcium silicate hydrate (Guan et al., 2013; Chen et al., 2013; Jiang et al., 2017; Fang et al., 2018). In addition, Fang et al. (2018) proposed that phosphate ions can diffuse through the surface of calcium silicate hydrate and replace the Ca-OH groups in the bulk solid with Ca-P groups. On the other hand, Okano et al. (2015) suggested that the prevalent mechanism of phosphate removal is not by precipitation with free Ca²⁺ released from calcium silicate hydrate, but by the formation of calcium-phosphate-silicate aggregates. Regardless of the mechanism, the concentration of Ca²⁺ in calcium silicate hydrate appears to strongly influence dissolved phosphate concentration.

In order to achieve higher concentration of Ca²⁺, previous studies have assessed synthesis parameters such as pH and temperature to obtain higher Ca/Si ratios in calcium silicate hydrate.

Studies have confirmed that synthesis pH >10 and a temperature of 100 °C lead to Ca/Si ratio ≥ 1 and more crystalline compounds in the resulting solid (Kuwahara et al., 2013). Cong and Kirkpatrick (1996) showed that the abundance of Ca-OH bonds increases with increasing Ca/Si ratio. On the other hand, faster release of Ca^{2+} was observed for poorly crystalline or amorphous forms rather than the crystalline forms of calcium silicate hydrate (Wan et al., 2005). Okano et al. (2013) synthesized an amorphous calcium silicate hydrate with a Ca/Si ratio of 2.0 by using alkali extraction of soluble silicates from a natural siliceous shale and mixing it with calcium hydroxide at a temperature of 60 °C. The resulting material showed on average 63% higher phosphorus removal than the crystalline form of calcium silicate hydrate. These observations were explored in this research to synthesize calcium silicate hydrate that can achieve higher phosphate removal.

The most common calcium phosphate mineral formed in phosphorus rich wastewaters is hydroxyapatite (Chen et al., 2009; Guan et al., 2012; Fang et al., 2018; Zhang et al., 2019) due to its thermodynamic stability (Drouet, 2013). Besides hydroxyapatite, tricalcium phosphate ($\text{Ca}_3(\text{PO}_4)_2$) and amorphous calcium phosphate ($\text{Ca}_x\text{H}_y(\text{PO}_4)_z \cdot n\text{H}_2\text{O}$, $n=3-4.5$) were also found to be formed during phosphate uptake (Chen et al., 2013; Zhang et al., 2019). According to Fang et al. (2018) both solution pH and Ca:P ratio are stronger predictors of which calcium phosphate species will be formed than the value of their solubility products.

In high alkalinity wastewaters, precipitation of calcium phosphate is greatly hindered by the presence of high concentration of bicarbonate and carbonate ions. Song et al. (2002) reported that with increasing carbonate concentration, Ca^{2+} ions form ion pairs with HCO_3^- and CO_3^{2-} rather than with PO_4^{3-} and the dissolved phosphate concentration increases. They also found that calcium phosphate can coprecipitate with calcite above pH 10 and the resulting solid phase is a mixture of

the two minerals, thereby decreasing the phosphorous density in the precipitated solid and making it unsuitable as a fertilizer substitute.

So far, the phosphate recovery performance of calcium silicate hydrate has been tested in synthetic anaerobic digestion liquor (containing 273 mg PO₄- P/L and 0.49 mg NH₃-N/L) without any carbonate (Okano et al., 2015) and in a secondary effluent of a biological sewage treatment plant containing 10 mg P/L and a dissolved organic carbon concentration of 6-12 mg/L (Berg et al., 2005). The alkalinity of anaerobically digested animal wastewaters can be as high as 4938±2304 mg/L as CaCO₃, most of which is due to high bicarbonate concentration (Huchzermeier and Tao, 2012). For practical application, the performance of calcium silicate hydrate needs to be evaluated in the same alkalinity range of animal wastewater. Also, the optimum pH ranges of maximum precipitation and dissolution of phosphate need to be identified to ensure effective phosphate uptake and subsequent release.

1.4 Phosphorus release from used calcium silicate hydrate

To be used as an efficient fertilizer, the applied phosphate must be available for plant growth. Due to frequent application of fertilizers, phosphorus adsorbs onto existing soil minerals or forms precipitates with free Al³⁺, Ca²⁺ and Fe³⁺ ions and removes available phosphate from soil solution into the soil solid phase, a process known as fixation (Barber, 1995). To estimate plant available phosphorus in soil, standard soil phosphorus tests have been developed to simulate soil root zone conditions, for example, using weak or dilute acid to model the acidic condition in the root zone caused by excretion of CO₂ (Dickman and Bray, 1941) or by microbially produced weak acids, such as acetic, malic, tartaric and oxalic acid which scavenge metal ions (Fe, Al, Ca, K, Mg) from soil minerals (Adeleke et al., 2017). Using these tests to extract phosphorus from used

calcium silicate hydrate can give insight into the processes responsible for phosphate uptake and release.

1.5 Hypotheses and objectives of this research

The first hypothesis of this research is that agricultural waste materials rich in silica can be utilized to synthesize calcium silicate hydrate for phosphorous uptake from wastewater. The second hypothesis is that high alkalinity of wastewater will interfere with the phosphorus uptake capacity of calcium silicate hydrate because the increased bicarbonate concentration will compete with phosphate to form calcium carbonate.

Based on the above hypotheses, the overall objective of this study was to evaluate the phosphate recovery performance of calcium silicate hydrate made from agricultural waste materials. The specific objectives were: 1) to identify suitable agricultural waste materials having high silica content and use them to synthesize calcium silicate hydrate 2) to maximize phosphate uptake capacity of these materials by inhibiting calcite formation 3) to examine effect of pH on phosphate uptake, 4) to examine effect of alkalinity by evaluating phosphate uptake in model wastewaters containing concentrations of typical anaerobic treatment effluent of dairy manure and 5) to evaluate phosphorus release from spent calcium silicate hydrate into modified extractants to understand the mechanisms behind phosphate uptake and release.

1.6 Thesis overview

Chapter Two contains the materials and methods used to synthesize and characterize calcium silicate hydrate, to measure phosphate uptake in deionized water and in model wastewater and to evaluate phosphorus release by modified methods of standard soil phosphorus tests. Chapter Three presents the results and the discussion of this research which include the selection of suitable agricultural waste material and appropriate synthesis parameters for calcium silicate hydrate so

that phosphate uptake can be maximized. The effect of pH and alkalinity were interpreted in terms of the solubility of different calcium phosphate minerals. Chapter Three also includes the results of phosphorus release from the precipitated solids in deionized water and model wastewater. Chapter Four lists the conclusions, recommendations for practice and future work. Appendix A contains procedures for preparation of standard phosphorus solutions and development of a calibration curve. Appendix B contains Scanning Electron Microscope (SEM) images of rice husk ash, rice straw ash and the calcite-tobermorite mixture prepared with the system open to the atmosphere. Appendix C summarizes preliminary experiments carried out with the calcite-tobermorite mixture which include phosphate uptake experiments at pH 7-10 and calculation of equilibrium calcium concentration from the solubility products of calcium phosphate minerals. Appendix D contains estimation of the production cost of calcium silicate hydrate from rice husk. It also includes the comparison of costs of one ton of phosphorus from calcium silicate hydrate and a commercial fertilizer – diammonium phosphate.

Chapter 2: Materials and Methods

2.1 Preparation of ash from rice husk and rice straw

All the reagents used in our experiments were of reagent or ACS grade and were used as received. Rice husk (E.C. Kraus flaked grain size rice husk) was bought from Home Brew Ohio, and rice straw (*Oryza sativa*, subspecies japonica) was provided by Dale Bumpers National Rice Research Center, Stuttgart, Arkansas, USA. At first, rice husk and straw were washed with deionized water and air dried for 24 hours. Then the samples were rinsed with 1 M HNO₃ (65-70%, Thermo Fisher Scientific, Waltham, MA) and again with deionized water until the pH increased to 6.3. After oven drying at 100 °C, the dried rice husk was placed in a crucible with an open lid to ensure presence of sufficient oxygen during heating so that the carbon produced from the decomposition of organic component of rice husk was removed as CO₂ (Glushankova et al., 2018). The crucible was placed inside an electric kiln (Paragon Caldera kiln, Paragon Industries, L.P., Mesquite, TX) and the rice husk was heated at a rate of 5 °C/min and held at 600 °C for 6 hours. The yield of ash, which is the weight percentage of material remaining after heating, was 18.8% and 9.5% for rice husk and rice straw, respectively.

2.2 Preparation of calcium silicate hydrate: Method 1

To dissolve the silica contained in the ash, an alkali leaching process was adopted that was described by Vaibhav et al. (2015). At first, three grams of ash were dissolved in 300 mL of 1 M NaOH (purity ≥97%, Thermo Fisher Scientific, Waltham, MA) in a beaker that was open to atmosphere and stirred at 400 rpm for 48 hours with a magnetic stir bar resulting in a solution pH of 13.9. Assuming the ash contained 95% silica (Chandrasekhar et al., 2003) and 100% dissolution, the concentration of dissolved silicate would be 0.158 M. However, the resulting solution was cloudy, so it is likely that not all of the silica from rice husk dissolved in NaOH. So, the

concentration of dissolved silicate could be lower than 0.158 M. To yield a Ca/Si ratio equal to or greater than 1:1 in the resulting material, a 300 mL solution of 0.158 M calcium nitrate ($\text{Ca}(\text{NO}_3)_2 \cdot 4\text{H}_2\text{O}$) (purity $\geq 99\%$, Thermo Fisher Scientific, Waltham, MA) was prepared to be mixed with the dissolved silicate. Before mixing with the dissolved silicate the pH of the calcium nitrate solution was adjusted to 11.0-11.2 using 1 M NaOH. The dissolved silicate was added dropwise into the calcium nitrate solution and was stirred with a magnetic stir bar for another 48 hours at 400 rpm in a beaker that was also open to atmosphere. The resultant slurry was washed three times with deionized water, then filtered and dried in the oven at 80 °C for 24 hours. X-ray diffraction (XRD) analysis of the dried material (Fig. 1a) showed significant presence of calcite (CaCO_3). As the system was open to atmosphere during the whole synthesis process, atmospheric CO_2 likely dissolved and transformed into other carbonate species at the high pH (13.9) of the solution that led to the formation of abundant calcite.

2.3 Preparation of calcium silicate hydrate: Method 2

To prevent the formation of calcite a revised procedure was used, in which ash from rice husk was dissolved in a 300 mL solution of 0.164 M NaOH in a glass bottle closed to the atmosphere, thus limiting the dissolution of atmospheric CO_2 . The concentration of NaOH required to dissolve the silica from the ash was determined experimentally by adding NaOH pellets into the solution until a clear solution was achieved. A different molarity of NaOH was used than the previous procedure to control the pH of the solution so that it is high enough (>12) to cause maximum dissolution of silica (Ayrál et al., 2008), but not unnecessarily high that could produce more carbonate in the system leading to formation of calcite. The dissolved silicate was added into pH adjusted (pH 11.0-11.2) 300 mL solution of 0.158 M calcium nitrate solution and the resultant slurry was washed and dried following the same procedures. The dried material was then ground

and sieved by a RX-20 Rotary Sifter between numbers 80 and 120 mesh sieves (0.177 mm and 0.125 mm) for 70 minutes. Unless otherwise noted, method 2 was followed to prepare calcium silicate hydrate for use in the experiments described below.

2.4 Material characterization

The morphology and chemical composition of ash from rice husk and rice straw and the calcium silicate hydrate synthesized open to atmosphere were analyzed by scanning electron microscopy with a energy-dispersive spectroscopy unit (SEM/EDS) (JEOL JSM-840A SEM) operated at 20 kV. The samples were sputter coated with gold and palladium before analysis. The crystalline phases of calcium silicate hydrate before and after phosphate uptake were examined by a Rigaku Ultima IV powder X-ray diffractometer with Cu K α radiation and Bragg–Brentano optics. XRD patterns were analyzed by Jade2010 software (Materials Data, Livermore, CA) and compared with Powder Diffraction Files (PDF) from the International Centre for Diffraction Data (ICDD).

2.5 Phosphorus uptake experiments

Batch tests were conducted to determine the phosphate uptake capacity of the prepared calcium silicate hydrate. For the uptake tests, three grams of calcium silicate hydrate per liter of phosphorus solution were used, with initial phosphorus concentrations varying from 0.69 to 68.5 mg P/L. The maximum initial concentration of 68.5 mg P/L was selected from the reported orthophosphate concentration in anaerobically digested dairy manure by Huchzermeier and Tao (2012). The pH of the reaction systems was adjusted using 5 M HCl (36.5-38%, Thermo Fisher Scientific, Waltham, MA) and 1 M NaOH solutions. Phosphorus solutions were prepared by dissolving NaH₂PO₄ (purity \geq 99%, Thermo Fisher Scientific, Waltham, MA) in deionized water. Phosphate uptake was also tested in a water system modeling the concentrations of certain

inorganic species: carbonate, ammonia, and phosphate in typical dairy wastewater (Huchzermeier and Tao, 2012). This model wastewater was prepared by dissolving 1.16 g of $(\text{NH}_4)_2\text{CO}_3$ (purity 99.99%, Alfa Aesar, Tewksbury, MA), 0.27 g of NaH_2PO_4 (purity $\geq 99\%$, Thermo Fisher Scientific, Waltham, MA) and 7.10 g of NaHCO_3 (purity 99.7 to 100.3%, Thermo Fisher Scientific, Waltham, MA) per liter of deionized water resulting in total ammonia concentration of 0.0241 M, phosphate concentration of 68.5 mg P/L and total alkalinity of 4723 mg/L as CaCO_3 at pH 8.0 (calculated in MINEQL+ 5.0, Hallowell, ME; ionic strength corrections were applied). Later a series of wastewaters was prepared with alkalinity values ranging from 100-700 mg/L as CaCO_3 , by varying the amount of NaHCO_3 and keeping the same ammonium concentration by adding 1.29 g of NH_4Cl (purity 99-100%, Mallinckrodt Baker, Inc, Phillipsburg, NJ) per liter of the wastewater. All samples were prepared in duplicate and were equilibrated on a reciprocal shaker with 30 excursions per minute for 24 hours. A preliminary kinetic test showed that the solution reached equilibrium within 24 hours. After equilibration, the samples were centrifuged for 30 minutes with a relative centrifugal force (RCF) of $2242\times g$ and 10 mL of supernatants were removed with Luer lock syringes and filtered through 0.22- μm filtration membranes (hydrophilic PVDF syringe filters, SIMSII Inc., Irvine, CA). The equilibrium phosphate concentration in the filtered liquids was determined by the standard ascorbic acid method (4500-P E., American Public Health Association, 1992) with the following modifications: (1) for phosphate determination in deionized water, a higher concentration of sulfuric acid (3.4 N) was used in the colorimetric reagent (Koenig et al., 2014) and (2) for phosphate determination in high alkalinity model wastewaters (4723-6120 mg/L as CaCO_3), 0.25% (w/v) oxalic acid (purity ≥ 99.5 , Thermo Fisher Scientific, Waltham, MA) was introduced into the samples before adding ascorbic acid as described in Galhardo and Masini (2000).

The first modification was done to avoid the interference of silica dissolved from calcium silicate hydrate during the colorimetric analysis of phosphate. In the standard ascorbic acid method, phosphate reacts with ammonium molybdate in acid medium to form phosphomolybdic acid while potassium antimonyl tartrate acts as a catalyst for this reaction. When silica is present in solution it also reacts with ammonium molybdate and forms silicomolybdic acid. Both phosphomolybdic and silicomolybdic acids can be reduced by ascorbic acid to form blue colored complex, which gives an overestimation of the phosphate in solution when determined colorimetrically. Using a more acidic colorimetric reagent generates the optimal pH that prevents formation of the competing blue colored complex from silicomolybdic acid, thus removing the interference from silica.

The second modification was done to avoid the heightened interference of silica due to high ionic strength and low $[H^+]/[MoO_4^{2-}]$ ratio of the samples caused by high alkalinity (Going and Eisenreich, 1973). By adding oxalic acid and ammonium molybdate before ascorbic acid, silicomolybdic acid is formed much more slowly than phosphomolybdic acid (Chalmers & Sinclair, 1966). So, when ascorbic acid is added, the blue complex formed is only due to the phosphorus concentration in the sample.

A UV-Vis dual beam spectrophotometer (Shimadzu UV-1601 spectrophotometer, Japan) was used to measure phosphorus concentration at 880 nm wavelength. Samples were analyzed with particle blanks in the reference cell of the spectrophotometer. Particle blanks were samples of phosphate-free deionized water or the model wastewater equilibrated with calcium silicate hydrate for 24 hours. Particle blanks were treated the same as samples (centrifugation, filtration and addition of colorimetric reagent) and were tested before each analysis. Any absorbance imparted by the particle blanks, due to presence of small particles that were not retained by filters,

was subtracted from the subsequent samples. Standard phosphate solutions were prepared from KH_2PO_4 (purity 98%, MilliporeSigma, Burlington, MA) and a six-point calibration curve was developed which is described in Appendix A. Calibration standards were analyzed during each experiment. The mass of phosphate removed was determined by the difference between initial and equilibrium phosphate concentrations of the samples.

To avoid contamination from any residual phosphorus, all glassware was first washed with tap water and phosphate-free detergent (Liquinox, White Plains, NY) and then rinsed nine times with deionized water. After washing, the glassware was soaked in 5% HCl solution overnight and dried in the oven. The spectrophotometer cuvettes were washed with deionized water five times after the testing of each sample and were soaked in 5% HCl when not in use.

2.6 Phosphorus release experiments

After withdrawing the supernatant for phosphate measurement, the remaining slurry of deionized water and model wastewater samples was filtered through Grade 5, Whatman, qualitative filter paper to collect the precipitated solids. A different size of filter paper than what used in phosphorus measurement was chosen for ease of filtration and on the basis of the assumption that most of the precipitated solids could be collected by it. Solids were collected from solutions where maximum phosphate uptake was observed (samples having initial phosphate concentration of 68.5 mg P/L and equilibrium pH of 9) to ensure detectable phosphorus in the solids (when analyzed by XRD) and in the extractants. After collecting the solids, they were air-dried for 48 hours. The same procedures were followed to collect and prepare solids for XRD analysis. Three common soil phosphorus tests (Mehlich 3, Bray P1 and Olsen) were used to gain insight on the phosphorus release potential of the collected solids. The compositions and the resulting pH of the extractants used in the tests are given in Table 1. All reagents listed in Table 1

were purchased from Thermo Fisher Scientific, Waltham, MA. The tests were carried out following the standard procedures described in Mehlich (1984), Bray and Kurtz (1945) and Olsen et al. (1954) with the following modifications: (1) the pH of Mehlich 3 extracting solution was adjusted from 2.3 to 7.0 using NH₄OH (ACS, 28.0-30.0% NH₃ basis, Sigma-Aldrich, St. Louis, Missouri) to represent neutral pH condition, (2) no soil was used in the tests and only a small amount of solid (0.025 g) was applied to the extractant (20 mL) to represent the phosphorus to extracting solution ratio in typical soil samples and (3) solids were shaken in Bray P1 extractant for 5 minutes instead of 1 minute as suggested by Pierzynski (2000). The solid shaking period for Mehlich 3 and Olsen test were 5 and 30 minutes, respectively as mentioned in the standard procedures (Mehlich, 1984; Olsen et al., 1954). A longer extraction time was suggested in the Olsen test to ensure the mixture reaches equilibrium and a good correlation is established between extracted and plant available phosphorus (Olsen et al., 1954).

Table 1 Composition of extractants used in Mehlich 3, Bray P1 and Olsen soil phosphorus tests.

Test Method	Composition of the extractant	pH of the extractant	pH of the extractant after adding solid
Mehlich 3	0.2 M CH ₃ COOH, 0.25 M NH ₄ NO ₃ , 0.015 M NH ₄ F, 0.013 M HNO ₃ , 0.001 M EDTA [(HOOCCH ₂) ₂ NCH ₂ CH ₂ N(CH ₂ COOH) ₂]	7.0 ¹	7.4-7.6
Bray P1	0.025 M HCl, 0.03 M NH ₄ F	2.5	3.5-3.6
Olsen	0.5 M NaHCO ₃	8.36	8.6

¹ Mehlich 3 extractant pH was adjusted from 2.3 to 7.0 using NH₄OH to represent the neutral pH condition of soil.

After mixing the extractnig solutions with the solids for the appropriate time, the solutions were separated from solid phase by filtering through 0.22- μm filtration membranes (hydrophilic PVDF syringe filters, SIMSII Inc., Irvine, CA). Phosphorus concentrations in the filtered solutions were measured by the second modified method with blanks in the reference cell, which were extractants without any solid in them. The released phosphorus (mg of P/g of solid) was calculated by the following formula:

$$\text{Phosphorus released } \left(\frac{\text{mg P}}{\text{g of solid}} \right) = \frac{C \times V}{M} \quad (1)$$

where C is the phosphorus concentration measured in extractant (mg P/L), V is the volume of extractant (0.02 L) and M is the mass of the solid added in extractant (0.025 g).

Chapter 3: Results and Discussion

3.1 Chemical composition of ash from rice husk and rice straw

To determine the silicon and arsenic content of ash from rice husk and rice straw, EDS analyses were conducted on ten different spots, randomly selected, in two separate samples of each material, and the results are shown in Table 2. For context, EDS cannot detect elements with atomic number less than 4 (i.e., hydrogen, helium and lithium) and trace elements with concentrations below 0.01% (wt%) (Nasrazadani and Hassani, 2016); so values reported in Table 2 should be viewed accordingly. The major elements present in both materials were carbon (C), oxygen (O) and silicon (Si). The C content of the rice straw ash sample was around 40%, which can be attributed to unoxidized carbon remaining after heating. The percentage of silicon in rice husk ash (83.0 ± 4.3 wt%) was significantly higher than in rice straw ash (20.7 ± 7.2 wt%) (Table 2), making it a good source of silica for calcium silicate hydrate synthesis.

In addition, the arsenic concentration in rice husk ash was below detection limits (< 0.01 wt%) while in rice straw ash it was 0.18 ± 0.06 wt% (Table 2). Previous studies also confirmed that arsenic accumulation in rice husk is at least one order of magnitude lower than in rice straw (Abedin et al., 2002; Rahman et al., 2007). So, using rice husk instead of rice straw in the preparation of calcium silicate hydrate reduces the risk of arsenic contamination in the treated water. Thus, due to its higher silicon and lower arsenic content, phosphate uptake and release experiments were carried out using calcium silicate hydrate made from rice husk ash.

Table 2 Composition¹ of ash from rice husk and rice straw based on EDS analysis.

Element	Rice husk ash (wt %)	Rice straw ash (wt %)
Si	83.0±4.3	20.7±7.2
As	Below detection limit	0.18±0.06
O	10.7±1.5	31.2±4.3
C	1.8±2.6	39±12
Ca	2.0±1.4	0.13±0.06
Mg	0.01±0.02	0.01±0.01
P	0.2±0.1	0.15±0.09
Cl	0.12±0.07	0.02±0.02
Na	0.01±0.14	0.05±0.03

¹ Each value reported consists of the mean and standard deviation of ten measurements carried out on ten different spots on two separate samples of each material.

3.2 Characterization of the synthesized calcium silicate hydrate

The XRD pattern of rice husk ash (Fig. 1b) consisted of a broad peak that ranged from 18 to 26° (2θ) which matches with opal (SiO₂·xH₂O, PDF#00-066-0178) (Fig. 1c), a hydrated amorphous form of silica. SEM images of rice husk ash and straw ash are shown in Fig. B.1 and B.2, respectively. The calcium silicate hydrate prepared from rice husk ash by keeping the system open to the atmosphere consisted of peaks that matched the XRD patterns of calcite (CaCO₃, PDF#98-000-0141), tobermorite (Ca₂Si₃O₁₁H₅, PDF# 98-000-8541) and silicon oxide (SiO₂ ITQ-07, PDF# 04-012-6672) (Fig. 1a). This material will be referred to as calcite-tobermorite mixture in the rest of the text. A SEM image of the calcite-tobermorite mixture is shown in Fig. B.3. A similar material was prepared using dissolved silica from rice straw ash (with system open to

atmosphere) and its SEM image is shown in Fig. B.4. The calcium silicate hydrate prepared by keeping the system closed to atmosphere (Fig. 1d) was mostly amorphous with one small peak at 29.5° (2θ). The location of the peak was matched with that observed in the XRD pattern of a metastable phase in the alkaline $\text{CaO-SiO}_2\text{-Al}_2\text{O}_3$ system and was identified as amorphous calcium silicate hydrate by Houston et al. (2009).

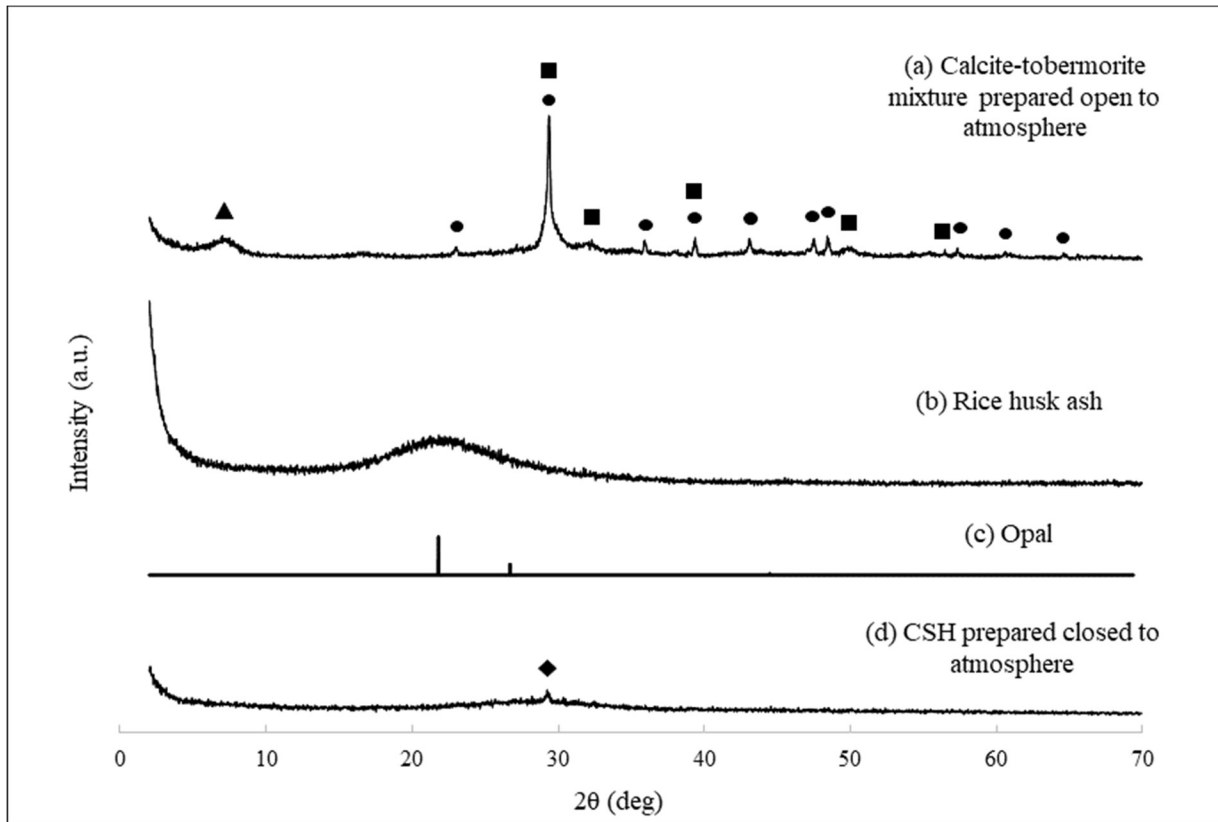


Fig. 1. XRD patterns of (a) calcite-tobermorite mixture synthesized with system open to atmosphere, (b) rice husk ash, (c) opal and (d) calcium silicate hydrate synthesized with system closed to atmosphere. Symbols: calcite (●), tobermorite (■), silicon oxide (SiO_2 ITQ-07) (▲) and calcium silicate hydrate-CSH (◆). The XRD patterns of opal, calcite, tobermorite and silicon oxide (SiO_2 ITQ-07) was obtained from the Powder Diffraction File database of International Center for Diffraction Data (ICDD). The peak location of calcium silicate hydrate was taken from Houston et al. (2009).

A comparison of the phosphate uptake capacities of calcite-tobermorite mixture and amorphous calcium silicate hydrate (Fig. 2) showed higher uptake (Q_e) for the latter material. One possible reason for low uptake by the calcite-tobermorite mixture could be the strong sequestration of Ca^{2+} in calcite which makes it less reactive than amorphous calcium silicate hydrate to form calcium phosphate. Preliminary experiments done with the calcite-tobermorite mixture are summarized in Appendix C. Other than Appendix C, the subsequent experiments were carried out with amorphous calcium silicate hydrate.

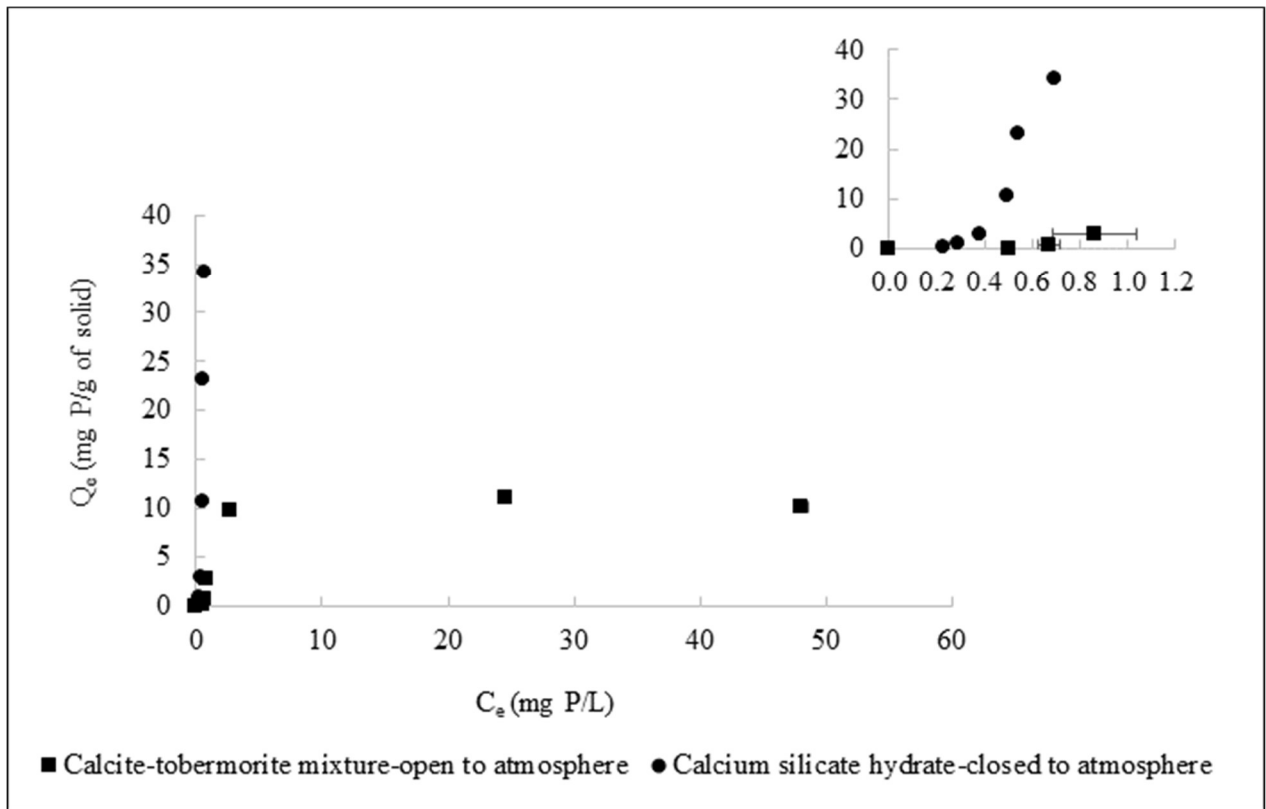


Fig. 2. Phosphate uptake by calcite-tobermorite mixture (synthesized open to atmosphere) and calcium silicate hydrate (synthesized closed to atmosphere). Material dosage and equilibrium pH were 2 g/L and 9, respectively. The inset panel indicates phosphate uptake at lower equilibrium phosphate concentrations. The error bars represent the standard deviations of the means associated with Q_e and C_e calculated from duplicate measurements.

3.3 Phosphorus uptake by calcium silicate hydrate

The phosphate uptake capacity of calcium silicate hydrate was tested in deionized water with initial phosphate concentrations (C_0) ranging from 0.69-68.5 mg P/L. Since phosphate is removed by reacting with Ca^{2+} from calcium silicate hydrate, increasing Ca^{2+} concentration is expected to achieve lower equilibrium phosphate concentration (C_e) which was confirmed by increasing the dosage from 2 g/L to 3 g/L. On average lower C_e values were achieved with the higher calcium silicate hydrate concentration (Fig. 3). No further increase of dosage was carried out to avoid the decrease in phosphorus content of the precipitated solids that could create a problem while reusing it as fertilizer.

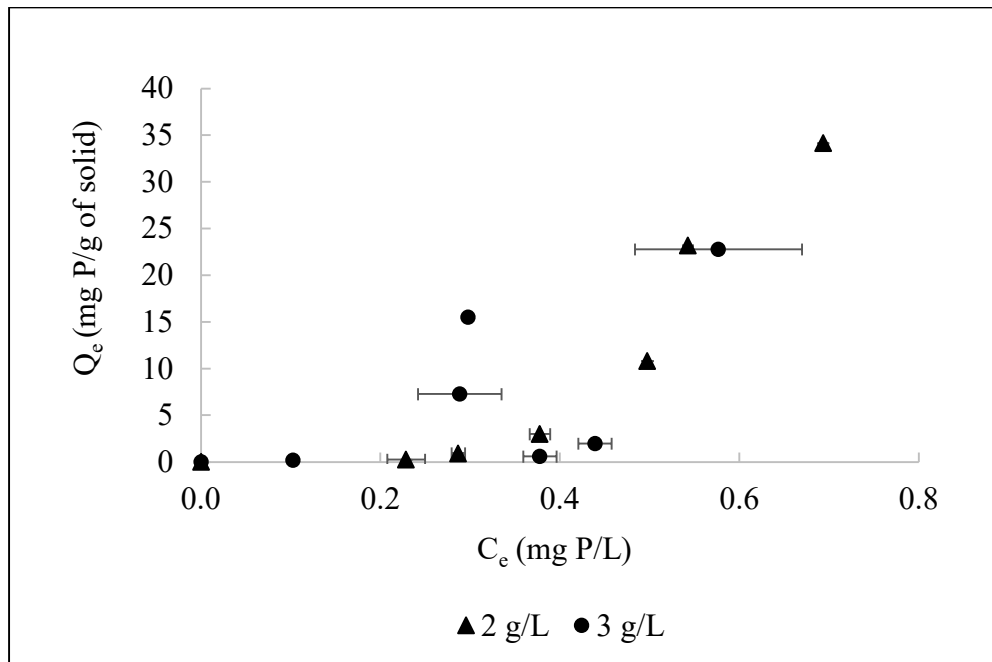


Fig. 3. Phosphate uptake by calcium silicate hydrate in deionized water with a dosage of 2 g/L and 3 g/L. The pH of the solutions was adjusted to 9. The error bars represent the standard deviations of the means associated with Q_e and C_e calculated from duplicate measurements. Large error bars for some data points could be due to the small sample size of 2 and/or the inhomogeneity of calcium silicate hydrate.

After selecting the appropriate dosage, the pH effect on phosphate uptake by calcium silicate hydrate was investigated. The lowest phosphate equilibrium concentration achieved was 0.58 ± 0.09 mg P/L (for initial concentration of 68.5 mg P/L) at pH 9, corresponding to a removal percentage of 99% (Fig. 4). By increasing pH from 8 to 9, $C_e < 1$ mg P/L and higher uptake (Q_e) were observed for every data point in the curve (Fig. 4 (inset)) which is not consistent with sorption of an anion (PO_4^{3-}). The surface charge of an adsorbent has the tendency to be less positive or more negative with increasing pH causing decrease in anion adsorption.

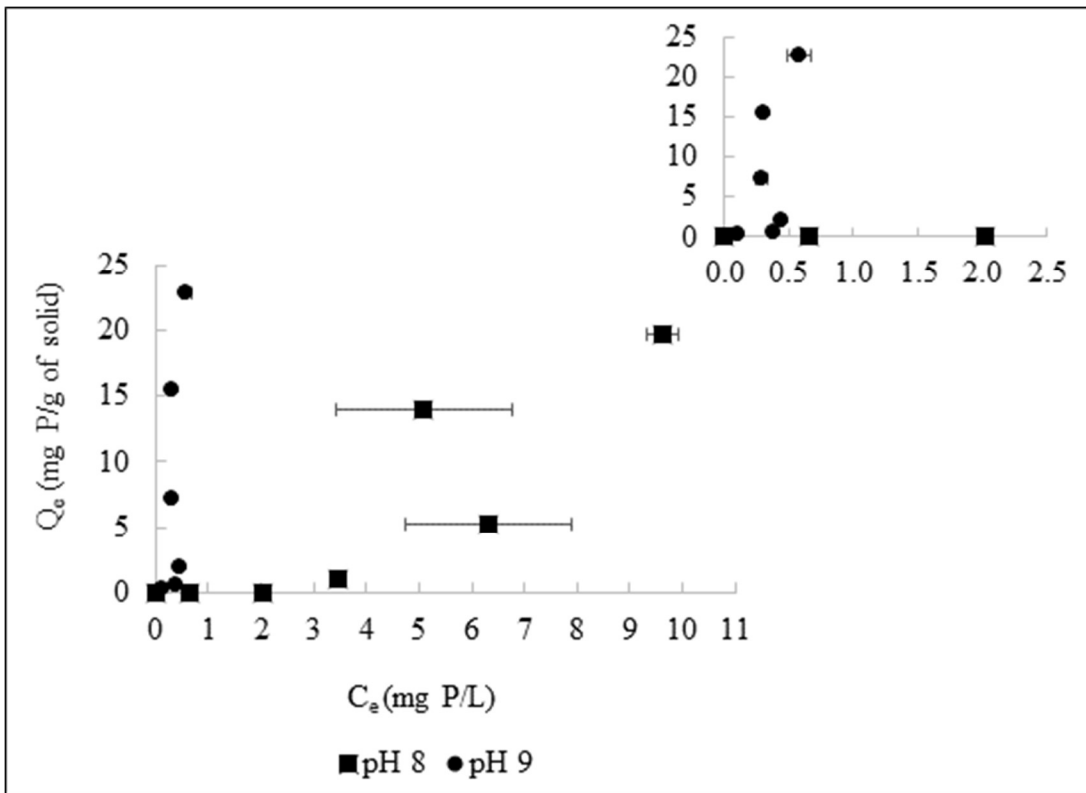


Fig. 4. Phosphate uptake by calcium silicate hydrate at pH 8 and 9 with a dosage of 3 g/L. The inset panel indicates phosphate uptake at lower equilibrium phosphate concentrations. The error bars represent the standard deviations of the means associated with Q_e and C_e calculated from duplicate measurements. Large error bars for some data points could be due to the small sample size of 2 and/or the inhomogeneity calcium silicate hydrate.

The increase in uptake observed from pH 8 to pH 9, can instead be explained by the precipitation of calcium phosphate minerals that typically form in anaerobically digested animal manure such as monetite (CaHPO_4), brushite ($\text{CaHPO}_4 \cdot 2\text{H}_2\text{O}$), hydroxyapatite ($\text{Ca}_5(\text{PO}_4)_3\text{OH}$), octacalcium phosphate ($\text{Ca}_8\text{H}(\text{PO}_4)_6 \cdot 3\text{H}_2\text{O}$) and β -tricalcium phosphate ($\beta\text{-Ca}_3(\text{PO}_4)_2$) (Gungor and Karthikeyan, 2008). Calcium phosphates like hydroxyapatite, β -tricalcium phosphate and octacalcium phosphate are less soluble at pH 9 than pH 8 (Fig. 5). So, the degree of supersaturation of the phosphate solutions is higher at pH 9 than at pH 8 with respect to these calcium phosphates and more phosphate is precipitated.

To further support the idea that phosphate is removed from the system by precipitation and not sorption, a qualitative analysis of the curves in Fig. 2, 3 and 4 was carried out. The curves show that at low equilibrium concentrations, there was little to no uptake of phosphate and C_e values were equal to C_0 (Fig. 2 inset, Fig. 3 and Fig. 4 inset). At high equilibrium concentrations, the curves did not reach a plateau suggesting uptake capacity of calcium silicate hydrate was limited but not completely exhausted (Fig. 2 inset, Fig. 3 and Fig. 4). Langmuir adsorption model was poor fit to the data both in low and high equilibrium concentration zones, as the model is based on the concept of highest uptake values at low equilibrium concentrations that plateau at high equilibrium concentrations due to filling up of all the adsorption sites. The overall shape of the uptake curves (Fig. 2 (inset), Fig. 3 and Fig. 4) suggest that at lower equilibrium concentration ranges (equilibrium concentrations of 0-0.2 mg P/L for Fig. 2 (inset), Fig. 3 and Fig. 4 (inset, pH 9) and 0-2 mg P/L for Fig. 4 (inset, pH 8)), there were not enough PO_4^{3-} ions to cause a supersaturation environment with respect to the relevant calcium phosphate mineral. One interpretation is that the ion activity product (IAP) of the calcium phosphate mineral to be formed was smaller than the solubility product (K_{sp}) of the same, which caused PO_4^{3-} ions to remain in the

dissolved phase. Similarly, at higher equilibrium phosphate concentration ranges (equilibrium concentrations >0.6 mg P/L for Fig. 2 (inset) and Fig. 3; >0.5 mg P/L (pH 9) and >9 mg P/L (pH 8) for Fig. 4), where the slope of the curves start to decrease, there was limitation of Ca^{2+} ions to form calcium phosphate precipitates.

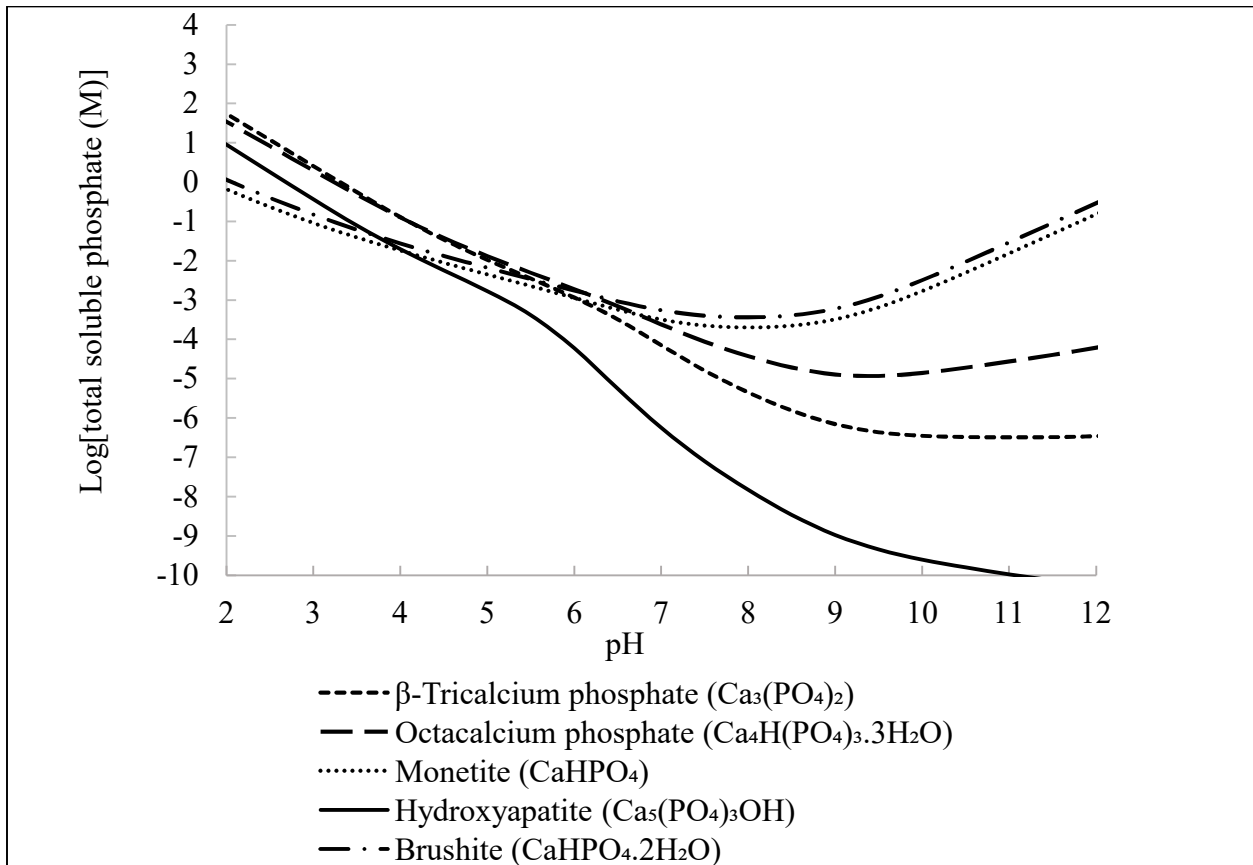


Fig. 5. Solubilities of calcium phosphate minerals calculated separately for each solid, with MINEQL+ version 5.0. Concentration of total calcium was assumed as 0.001 M and phosphate solubility was controlled by the mineral/water equilibrium. Formation constants of all minerals were from MINEQL+ database.

Calcium silicate hydrate made from rice husk was able to remove 99% of the initial phosphate concentration of 68.5 mg P/L at pH 9 (Fig. 4) in solutions of deionized water, which is higher than the phosphorus removal achieved by struvite (70-82%), biological processes (80-90%)

and other synthesized calcium silicate hydrates (54-95%) (Morse et al., 1998; Qureshi et al., 2006; Le Corre et al., 2009; Guan et al. 2013; Okano et al. 2013; Kuwahara et al., 2013; Jiang et al., 2017; Lee et al., 2018; Fang et al., 2018). However, the higher phosphorus removal by our material was achieved in ideal water conditions i.e., without the presence of typical constituents of wastewater, which is not realistic. So next, the performance of calcium silicate hydrate was tested in a simplified model wastewater containing concentrations of total ammonia and total alkalinity similar to anaerobic treatment effluent of dairy manure (Huchzermeier and Tao, 2012). At first, phosphate uptake in the model wastewater was studied at pH 8, 9 and 10. The total alkalinity of the model wastewater increased from 4723-6120 mg/L as CaCO_3 as pH was increased from 8-10, due to the increased concentration of carbonate ions which contribute to alkalinity twice as much as bicarbonate for the same concentration. Phosphate uptake in these high alkalinity wastewaters was significantly lower than in the system with zero alkalinity, i.e., in deionized water. The highest uptake achieved in the model wastewater was 5.3 ± 0.8 mg P/g of solid (for an initial concentration of 68.5 mg P/L) at pH 9 which was 77% lower than that observed in deionized water (compare Fig. 4 and Fig. 6). This is attributed to the ion pair complexes between Ca^{2+} and $\text{HCO}_3^-/\text{CO}_3^{2-}$ which become the predominant calcium-containing species at high carbonate levels (0.05 M) and at pH >8.5 (Ferguson and McCarty, 1969) and precipitate calcite ($\text{CaCO}_{3(s)}$) instead of calcium phosphate.

Phosphate uptake in the model wastewater at pH 8 and 9 was quite similar but was much lower at pH 10 as no phosphate was taken up below the initial concentration of 22 mg P/L (corresponding equilibrium concentration 21.6 ± 0.1 mg P/L) (Fig. 6). The higher fraction of carbonate concentration at pH 10.3 resulted in more precipitation of calcite. It decreased the amount of free Ca^{2+} ions to the point that no calcium phosphate is precipitated.

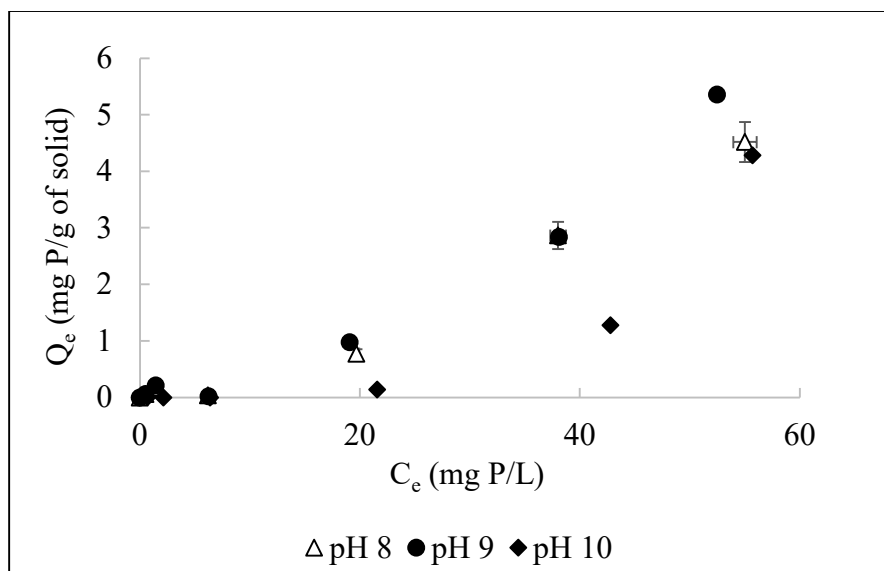


Fig. 6. Phosphate uptake by calcium silicate hydrate in model dairy wastewater at pH 8, 9 and 10. Total alkalinity of the wastewater was calculated to be 4723, 5000 and 6120 mg/L as CaCO_3 at pH 8, 9 and 10, respectively (by applying ionic strength corrections in MINEQL+ version 5.0). The error bars represent the standard deviations of the means associated with Q_e and C_e calculated from duplicate measurements.

Formation of calcite was visible in the XRD results of the precipitated solids collected from model wastewater before and after reacting with phosphorus (Fig. 7a and b). Peaks of calcite was also found in the XRD patterns of precipitated solids in deionized water before and after reacting with phosphorus (Fig. 7c and d), indicating the natural transformation of calcium silicate hydrate to calcite in presence of atmospheric CO_2 (Li et al., 2020). However, it is likely that due to the high carbonate concentration much more calcite was formed in model dairy wastewater than in deionized water which hindered the phosphate uptake.

Besides the peaks that were detected as calcite, the XRD patterns of solids collected from all four systems contained two additional peaks at 38.3 and $44.4^\circ 2\theta$ that could not be identified (Fig. 7a, b, c and d). No characteristic peaks of crystalline calcium phosphate phases were observed

for solids collected after reacting with phosphorus (Figures 7b and 7d), which means the formed calcium phosphates might be poorly crystalline or amorphous in nature or they were below detection limits.

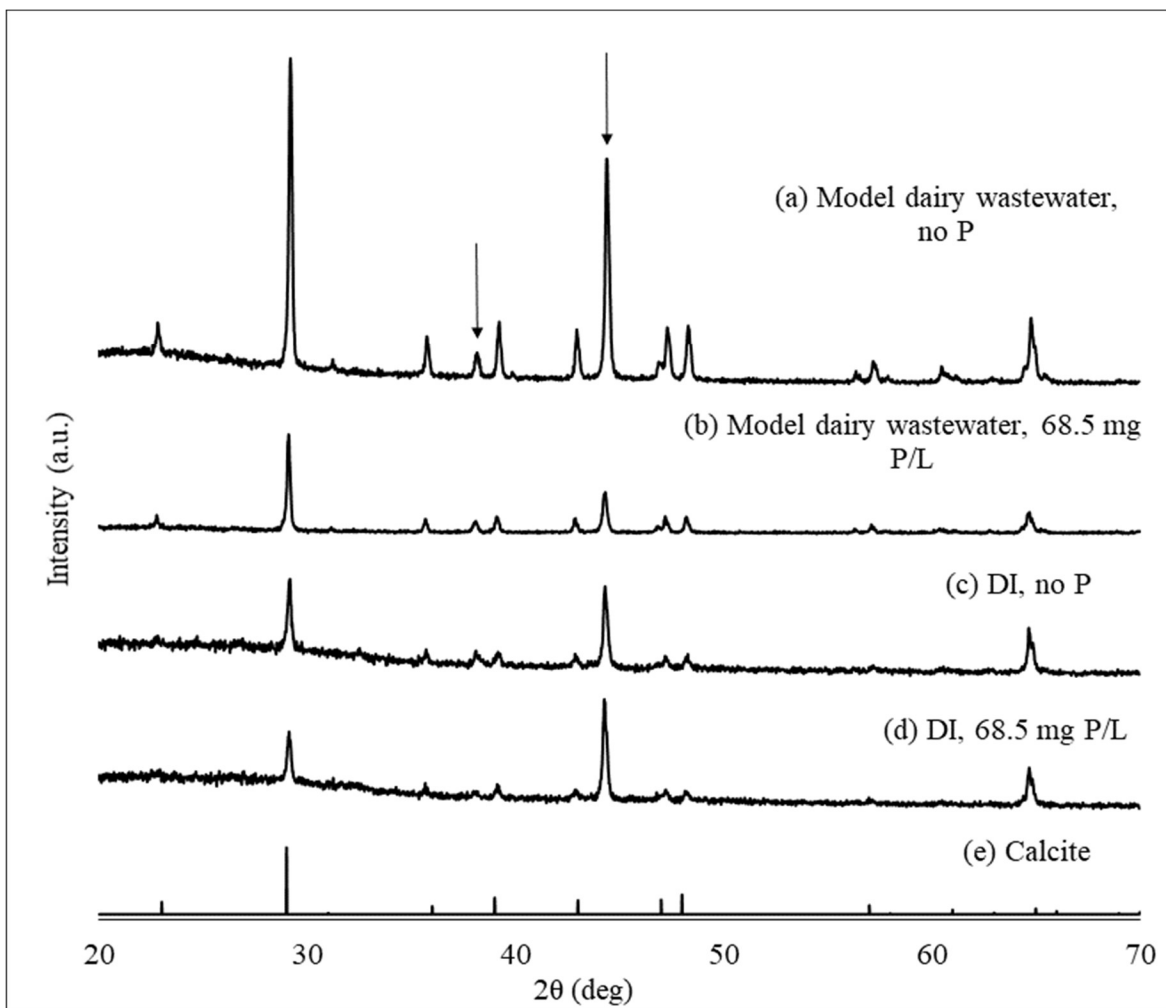


Fig. 7. XRD patterns of precipitated solids collected from (a) model dairy wastewater with no phosphate, (b) model dairy wastewater with 68.5 mg P/L (c) deionized water with no phosphate (d) deionized water with 68.5 mg P/L and (e) XRD pattern of calcite obtained from the Powder Diffraction File database of International Center for Diffraction Data (ICDD). The arrows indicate unidentified peaks. All solutions mentioned above were adjusted to pH 9.

To gain insight into which calcium phosphate species precipitated during phosphate uptake, the dissolved calcium concentration in the deionized water-calcite-tobermorite system was measured and compared with the calculated dissolved calcium concentrations in equilibrium with each of the following calcium phosphate minerals: brushite, monetite, hydroxyapatite, octacalcium phosphate and β -tricalcium phosphate (Appendix C). Among these, the calcium concentrations calculated for monetite and brushite were the closest to measured data (Fig. C.1), suggesting that monetite and/or brushite might have formed during phosphate uptake by calcite-tobermorite mixture. Similar calculations and comparison with experimental data could indicate which calcium phosphate species precipitated during phosphate uptake by the amorphous calcium silicate hydrate.

Next, a series of model wastewaters was prepared by varying the total alkalinity from 100 to 5000 mg/L as CaCO_3 at pH 9 and the phosphate uptake trend of calcium silicate hydrate was observed in these systems. The purpose of this set of experiments was to determine an alkalinity level where phosphate uptake by calcium silicate hydrate is no longer hindered by the formation of calcium carbonate. By decreasing alkalinity from 5000-100 mg/L as CaCO_3 , phosphate uptake increased proportionately. Uptake in model wastewaters with 100, 200 and 300 mg/L as CaCO_3 alkalinity were not significantly different from that achieved in deionized water (no added alkalinity) (Fig. 8 (inset)). For the initial concentration of 68.5 mg P/L, the equilibrium concentrations achieved in deionized water, 100, 200 and 300 mg/L alkalinity systems at pH 9 were 0.58 ± 0.09 (Fig. 4), 0.58 ± 0.14 , 0.48 ± 0.18 and 0.48 ± 0.19 mg P/L, respectively (Fig. 8) indicating >99% removal of phosphorus in all these conditions.

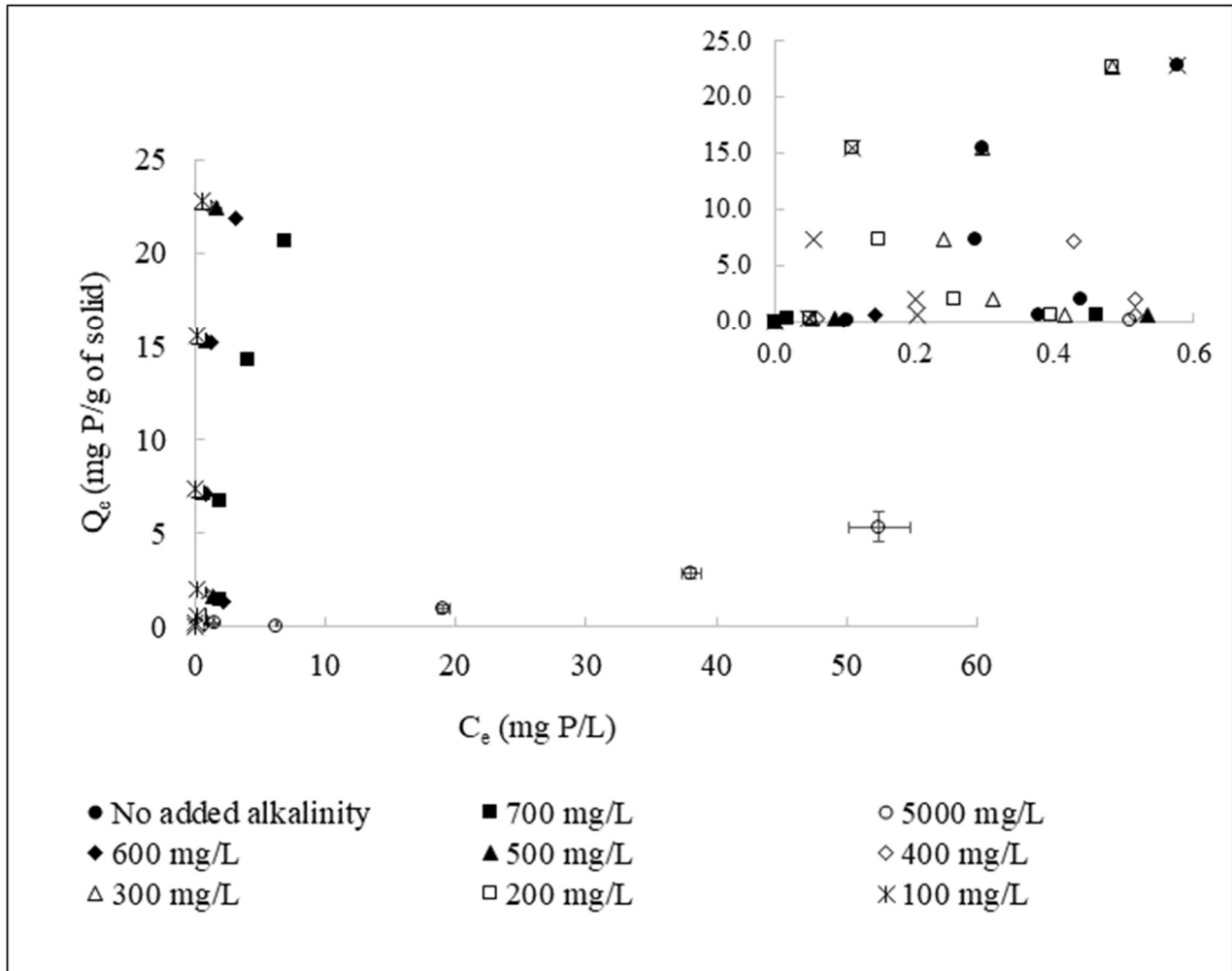


Fig. 8. Phosphate uptake by calcium silicate hydrate in model wastewaters containing total alkalinity ranging from 0-5000 mg/L as CaCO_3 at pH 9. Inset panel indicates phosphate uptake in wastewaters containing 0-300 mg/L as CaCO_3 at pH 9. The error bars represent the standard deviations of the means associated with Q_e and C_e calculated from duplicate measurements. Error bars are not shown for the data in the inset so the trends could be illustrated more clearly.

3.4 Phosphorus release by spent calcium silicate hydrate

To get insight into the phosphorus release capacity of spent calcium silicate hydrate, precipitated solids from solutions of deionized water and model dairy wastewater (initial phosphate concentration 68.5 mg P/L, pH 9) were collected. Phosphorus contained in the

precipitated solids was extracted by the modified Mehlich 3, Bray P1 and Olsen tests mimicking the conditions of neutral, acidic, and alkaline soils, respectively and the results are shown in Fig. 9.

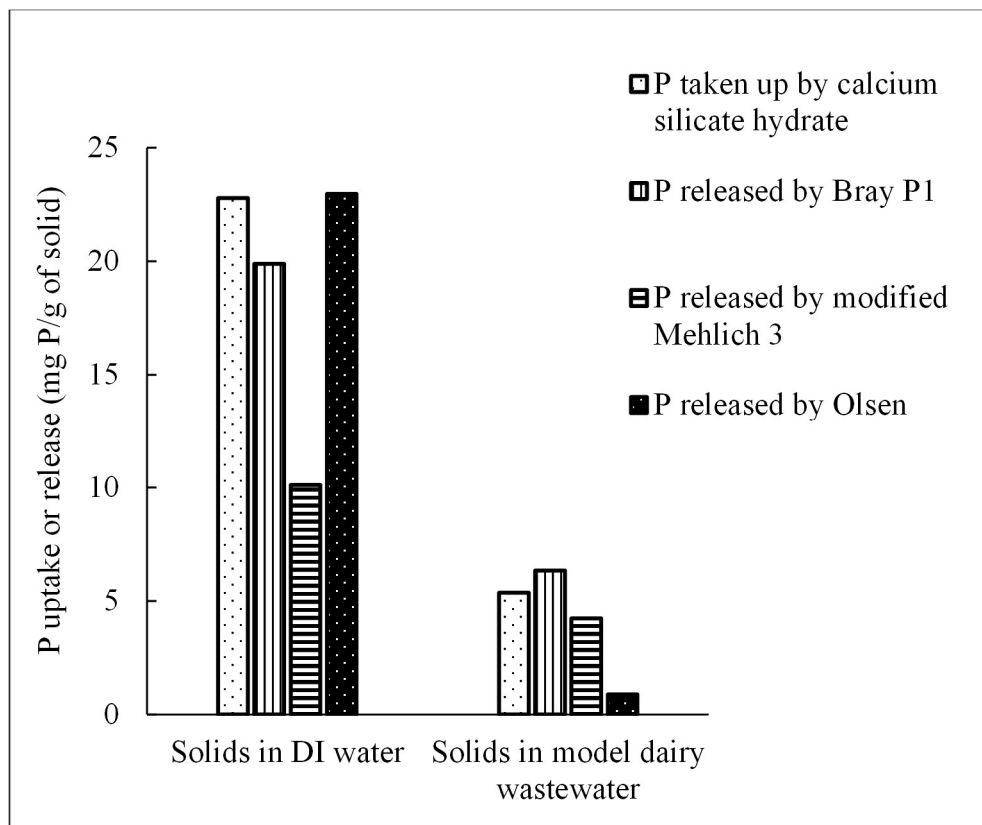


Fig. 9. Phosphorus release by precipitated solids collected from phosphate solutions of deionized water and model dairy wastewater (initial phosphate concentration 68.5 mg P/L). Solid to extractant ratio was 1:800 (w/v). The relative standard deviation ranged from 1-4% for measurements made in standard solutions of NaH_2PO_4 .

For solids collected from deionized water, phosphorus released in Bray P1 and Olsen extractant were higher than that in Mehlich 3. Extractants used in Bray P1 and Mehlich 3 methods both contain F^- (as NH_4F), that reacts with Ca^{+2} and drives the dissolution of calcium phosphate minerals (Dickman and Bray 1941; Mehlich, 1984). In this study, the Mehlich 3 extracting solution

was modified to neutral pH, whereas the Bray P1 extractant had a considerably lower pH. Under these conditions, the neutral ammonium fluoride in Mehlich 3 method measured only the adsorbed form of phosphorus, while Bray P1 estimated the sum of acid-soluble or mineral phosphorus and the adsorbed phosphorus. The extractant used in Olsen test consists of 0.5 M HCO_3^- (as NaHCO_3) which reacts with Ca^{2+} and moves the phosphate from the solid phase to solution. It also estimates the concentrations of both mineral (HCO_3^- soluble) and adsorbed forms of phosphorus. The low amount of adsorbed phosphorus released in modified Mehlich 3 extractant suggests that most of the phosphorus removed from deionized water was by precipitation and not adsorption.

We expected to see a similar trend in phosphorus release for the solids collected from model wastewater. But for these solids, phosphorus released in Olsen test was lower than Bray P1 and modified Mehlich 3 tests. One possible reason could be that the high concentration of bicarbonate in model wastewater system already mobilized the HCO_3^- soluble phosphorus, and the remaining phosphorus in the solids was mostly of the adsorbed form.

3.5 Cost comparison of calcium silicate hydrate with commercially available fertilizer

The total cost of production of calcium silicate hydrate made from rice husk was found to be \$464/ton (Table D.1) which is comparable to the \$410/ton price of commercially available diammonium phosphate fertilizer (DAP). While costs of the two materials are fairly similar, due to its low phosphorus density, the amount of calcium silicate hydrate required to yield one ton of phosphorus is 6.7-10.2 times higher than that of DAP (Table D.2). This resulted in a cost of \$14,000-20,000 to provide one ton of phosphorus from calcium silicate hydrate whereas for DAP fertilizer the cost is \$1800.

To compete with commercially available fertilizers, the cost of one ton of phosphorus from calcium silicate hydrate needs to be reduced which could be achieved by adopting one/both of the

following steps: 1) reducing the overall production cost by using significantly less expensive chemicals and 2) increasing the phosphorus concentration in calcium silicate hydrate. The first step could be carried out by replacing the most expensive chemicals used in the preparation of calcium silicate hydrate, i.e., calcium nitrate and sodium hydroxide with less expensive reagents such as lime. It was estimated that by using lime the cost of one ton phosphorus from calcium silicate hydrate was reduced to \$2200-3300, which is an 84% decrease from the previous price (Table D.3). To increase the phosphorus density in calcium silicate hydrate the solid to solute ratio could be decreased and/or a mesoporous calcium silicate hydrate can be synthesized for increased dissolution of Ca^{2+} and higher precipitation of phosphate, which will be the focus of future research.

Chapter 4: Conclusions and Recommendations

4.1 Conclusions

Using silica-rich agricultural waste materials (e.g. rice husk and rice straw), calcium silicate hydrate was prepared to recover phosphate from wastewater. While both materials showed potential for recovering phosphorus, rice husk was preferable over rice straw due to high silicon and low arsenic content. Limiting formation of calcite by closing the system to the atmosphere during synthesis led to a less crystalline and better performing calcium silicate hydrate that achieved 99% phosphate removal from solutions of deionized water at pH 9 (for initial concentration of 68.5 mg P/L and a dosage of 3 g/L). The increase of uptake observed from pH 8 to 9 was not consistent with adsorption but could be explained by the pH-dependent solubilities of certain calcium phosphates (hydroxyapatite, β -tricalcium phosphate and octacalcium phosphate). Besides pH, phosphate removal depended on the availability of free Ca^{2+} ions released from calcium silicate hydrate and the PO_4^{3-} ions in wastewater to precipitate one or more calcium phosphate minerals. The phosphate uptake capacity of calcium silicate hydrate was greatly impaired in water systems containing high alkalinity similar to animal wastewaters due to HCO_3^- and CO_3^{2-} competing with HPO_4^{2-} to form ion pairs and precipitating calcium carbonate instead of calcium phosphate. When alkalinity was lowered to 100-300 mg/L as CaCO_3 , the phosphate uptake was similar to that achieved with deionized water systems.

Phosphorus laden solids collected from deionized water and model wastewater were evaluated for phosphorus release using modified Mehlich 3, Bray P1 and Olsen tests. For solids collected from deionized water, the amount of phosphorus released in modified Mehlich 3 test was lower than that in Bray P1 and Olsen tests. This was attributed to the extraction of only adsorbed

phosphorus by modified Mehlich 3 extractant, whereas Bray P1 and Olsen extractants estimated the sum of mineral and adsorbed forms. This also indicated that most of the phosphate in deionized water was not removed by adsorption, but through precipitation of calcium phosphate. For solids collected from model wastewater, Olsen extractant was unable to mobilize HCO_3^- soluble phosphorus due to the increased concentration of bicarbonate prevailing in the system.

The cost to produce enough calcium silicate hydrate to yield one ton of phosphorus was estimated to be 6.7 to 10 times higher than the commercially available DAP fertilizer due to the low phosphorus density in calcium silicate hydrate and the high chemical costs of calcium nitrate and sodium hydroxide. Preliminary calculations showed that using lime instead of calcium nitrate and sodium hydroxide could reduce the cost of calcium silicate hydrate by 84% making its price comparable to DAP.

4.2 Recommendations for practice

For application of calcium silicate hydrate as a potential phosphorus recovery and reuse product, the following recommendations are proposed:

1. In this study rice husk ash was chosen to synthesize calcium silicate hydrate due to its low arsenic and high silicon content. As bioaccumulation of arsenic in rice plants vary depending on the arsenic content of soil and irrigation water and on the nature of rice species, chemical composition of the rice husk to be used needs to be carefully inspected before introducing in water treatment (Islam et al., 2016).
2. Less expensive materials like lime can be used instead of calcium nitrate and sodium hydroxide to synthesize calcium silicate hydrate.
3. It was found that lowering the alkalinity of model wastewater improved the phosphate uptake capacity of calcium silicate hydrate. Low cost methods of alkalinity reduction such

as excess aeration (Davis et al., 1991) or nitrification via biological treatment (Vanotti et al., 2003) are recommended prior to treating animal wastewater with calcium silicate hydrate for significant phosphorus removal.

4.3 Recommendations for future research

Building upon the findings of this work, the following recommendations are made for future research:

1. Other agricultural waste materials that are rich in silica and abundant in different parts of the world (e.g. corn cob and stalk, wheat hull, sugarcane and sorghum bagasse, peanut shells, palm husk and kernel shell and bamboo leaves (Terzioğlu et al., 2013; Aprianti et al., 2015; Mupa et al., 2015; Roselló et al., 2015; Permatasari et al., 2016; Yao et al., 2016; Memon et al., 2020) – should be tested to synthesize effective calcium silicate hydrate and their phosphate uptake capacities need to be evaluated.
2. Future research should also focus on enhancing the phosphate removal capacity of calcium silicate hydrate by synthesizing samples with higher surface area that can dissolve faster, release more Ca^{2+} and precipitate more phosphate from wastewater.
3. The phosphorus laden calcium silicate hydrate needs to be tested in realistic soil conditions containing Al and Fe minerals that have the potential to react with soluble phosphorus and hinder its availability to plants.
4. Detailed life cycle assessment needs to be carried out to determine whether the process of recovering phosphorus from wastewater by calcium silicate hydrate and reusing it as a fertilizer is environmentally more sustainable than the production of commercial fertilizers from phosphate rock.

Appendix A: Preparation of calibration standards

1. A concentrated stock solution of 50 mg P/L was prepared by adding 0.2195 g anhydrous KH_2PO_4 to 1 L of deionized water. To make it anhydrous, the KH_2PO_4 was dried overnight at 105 °C and stored in a desiccator.
2. This concentrated solution was diluted to 1 mg P/L standard which was used to make a series of less concentrated standards of 0.01, 0.05, 0.1, 0.2 and 0.5 mg P/L in 25 mL bottles. An example of a calibration curve is shown in Fig. A.1.
3. Standards were prepared weekly and tested before each experiment.

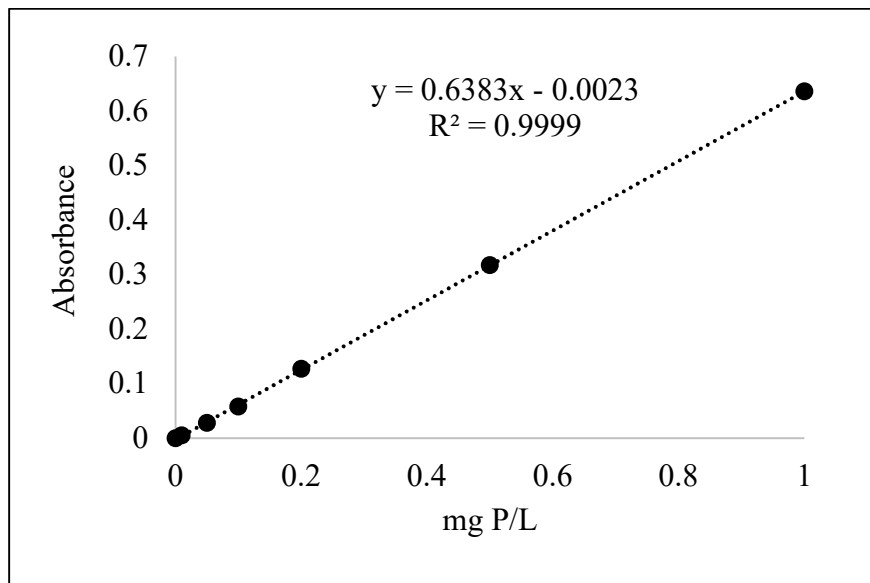


Fig. A.1 Example of a calibration curve.

Appendix B: SEM images of rice husk ash, rice straw ash and calcium silicate hydrate (calcite-tobermorite mixture)

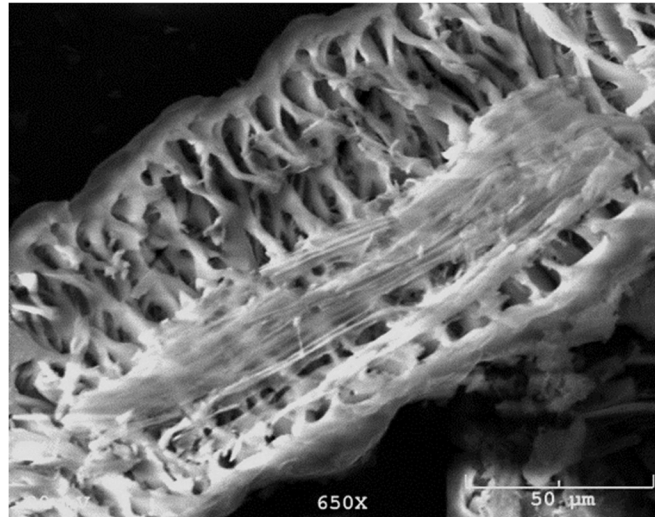


Fig. B.1. SEM image of rice husk ash.

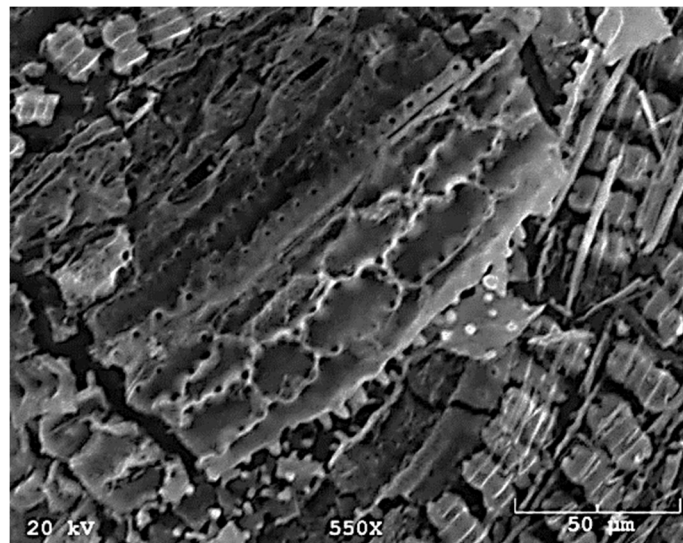


Fig. B.2. SEM image of rice straw ash.

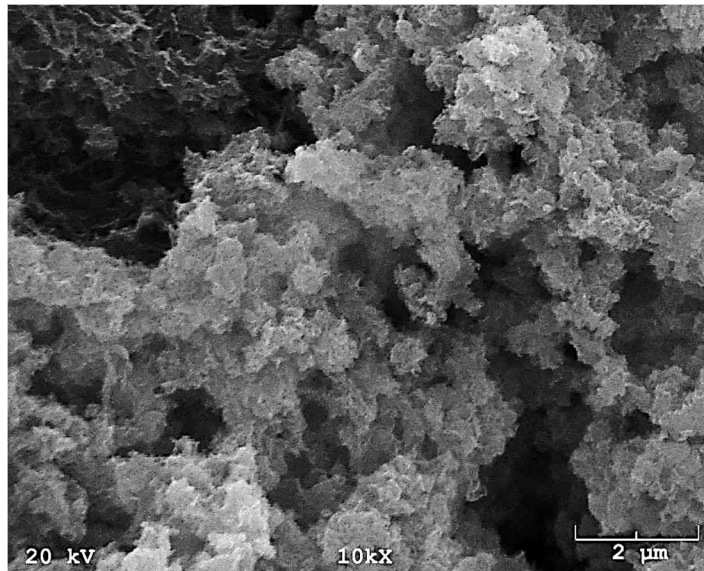


Fig. B.3. SEM image of calcite-tobermorite mixture made from rice husk ash (synthesized with system open to atmosphere).

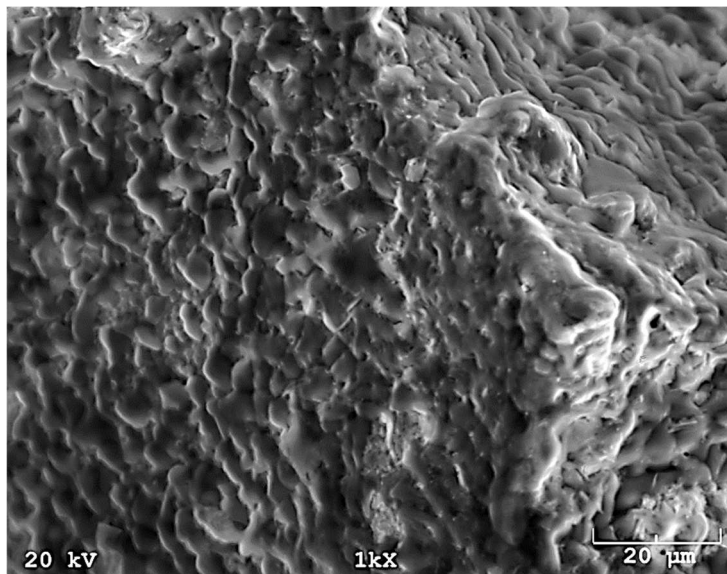


Fig. B.4. SEM image of calcium silicate hydrate made from rice straw ash (made with system open to atmosphere).

Appendix C: Preliminary experiments done with calcite-tobermorite mixture

This appendix summarizes the preliminary experiments done with calcite-tobermorite mixture which was synthesized by keeping the system open to atmosphere. The first part of this appendix includes phosphate uptake experiments at pH 7, 8, 9 and 10 in deionized water with a dosage of 2 g/L. The second part consists of calculation of theoretical calcium concentration from the solubility products of certain calcium phosphates to understand which calcium phosphate minerals could have formed during uptake. These experiments were performed before preparing the calcium silicate hydrate with limited exposure to CO₂, which was more effective at phosphate uptake.

The highest amount of phosphate uptake by the calcite-tobermorite mixture was seen at pH 8 ($Q_e = 20.71 \pm 0.71$ mg of P/g of solid, initial concentration = 68.5 mg P/L) (Fig. C.1). At higher equilibrium concentrations of phosphate (11.6-50.7 mg P/L), the uptake capacity did not show any trend with increasing pH. At the lower initial concentration range (0.3-2.3 mg P/L), phosphate uptake at pH 9 and 10 were quite similar and at pH 7 and 8 the trend was pH 8 > pH 7 (Fig. C.1 inset).

The better uptake of phosphate at pH 8 than at pH 9 and 10 can be explained by the formation of one or more calcium phosphate minerals that has lower solubility at pH 8 than at pH 9 and 10. To get an insight into which calcium phosphate minerals might have formed, the equilibrium Ca²⁺ concentrations were measured in selected samples of deionized water-calcite-tobermorite system (initial phosphate concentrations of 22, 46.5 and 68.5 mg P/L) at pH 10. Dissolved calcium concentrations were measured using the standard method for calcium determination (Test Method A, ASTM D511-03, 2003), which is based on the complexation chemistry between Ca²⁺ and EDTA.

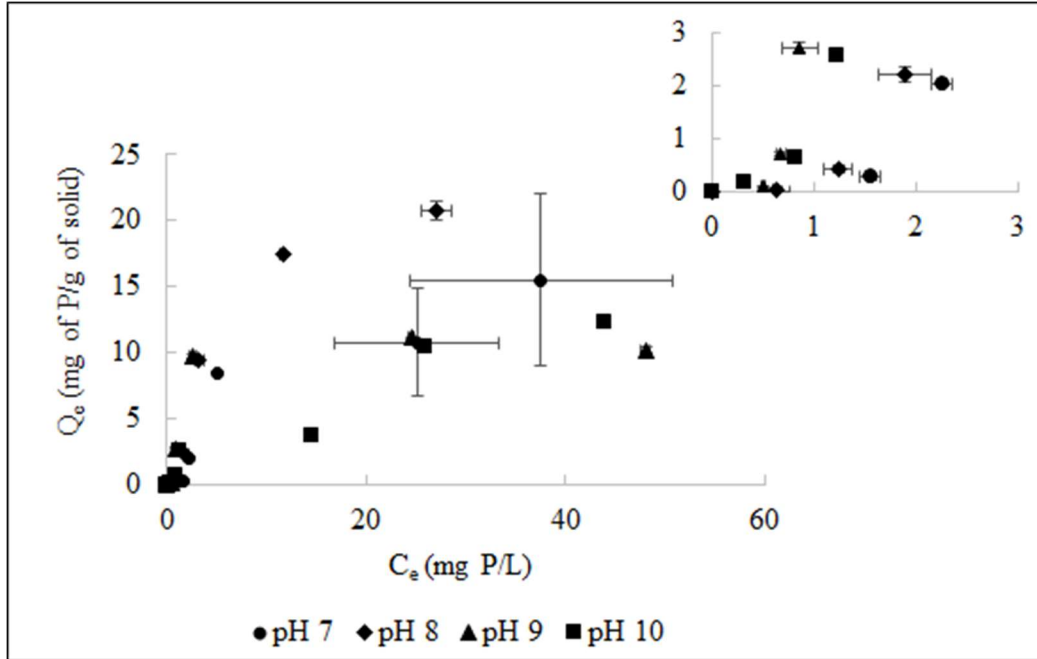


Fig. C.1. Phosphate uptake by calcite-tobermorite mixture at pH 7, 8, 9 and 10 with initial phosphate concentrations of 0.69-68.5 mg P/L and dosage 2 g/L. The inset panel indicates phosphate uptake at lower equilibrium phosphate concentrations. The error bars represent the standard deviations of the means associated with Q_e and C_e calculated from duplicate measurements.

In addition, Ca^{2+} concentrations were calculated theoretically from the solubility products (K_{sp}) of the following calcium phosphate minerals which are typically found in anaerobically digested manure: brushite ($CaHPO_4 \cdot 2H_2O$), monetite ($CaHPO_4$), octacalcium phosphate ($Ca_4H(PO_4)_3 \cdot 3H_2O$), β -tricalcium phosphate ($\beta-Ca_3(PO_4)_2$) and hydroxyapatite ($Ca_5(PO_4)_3OH$) (Gungor and Karthikeyan, 2008). The K_{sp} values of the minerals were taken from Dorozhkin (2007). A sample calculation of theoretical Ca^{2+} concentration from the K_{sp} value of monetite is shown below:

$$K_{sp(CaHPO_4)} = [Ca^{2+}] \times [H^+] \times [PO_4^{3-}] \quad (\text{at } 25^\circ C) \quad (C1)$$

Therefore,
$$[\text{Ca}^{2+}] = \frac{K_{sp}}{[\text{H}^+] \times [\text{PO}_4^{3-}]} \quad (\text{C2})$$

Where $[\text{H}^+]$ (mol/L) is calculated from measured equilibrium pH and $[\text{PO}_4^{3-}]$ (mol/L) is the concentration of PO_4^{3-} species present at pH 10 (a fraction of the total orthophosphate measured experimentally).

The value of $[\text{PO}_4^{3-}]$ at pH 10 was calculated as follows:

At pH 10, dominant species of phosphoric acid are HPO_4^{2-} and PO_4^{3-} .

So, the measured equilibrium concentration of total orthophosphate,

$$C_e \text{ or } C_T = [\text{HPO}_4^{2-}] + [\text{PO}_4^{3-}] \quad (\text{C3})$$

$$\text{The third ionization fraction of phosphoric acid is, } \alpha_3 = \frac{K_{a1} \times K_{a2} \times K_{a3}}{D} \quad (\text{Jensen, 2003}) \quad (\text{C4})$$

where, $K_{a1} = 7.5 \times 10^{-3}$, $K_{a2} = 6.2 \times 10^{-8}$ and $K_{a3} = 1.7 \times 10^{-12}$ are dissociation constants of phosphoric acid (H_3PO_4), H_2PO_4^- and HPO_4^{2-} , respectively (Jensen, 2003).

$$\text{and } D = [\text{H}^+]^3 + [\text{H}^+]^2 \times K_{a1} + [\text{H}^+] \times K_{a1} \times K_{a2} + K_{a1} \times K_{a2} \times K_{a3} \quad (\text{Jensen, 2003}) \quad (\text{C5})$$

$$\text{Also, } \alpha_3 = \frac{[\text{PO}_4^{3-}]}{C_T} \quad (\text{Jensen, 2003}) \quad (\text{C6})$$

$$\text{So, } [\text{PO}_4^{3-}] = \alpha_3 \times C_T \quad (\text{C7})$$

Using the concentration of PO_4^{3-} (from equation C7) and the individual K_{sp} value of the above mentioned calcium phosphates, the theoretical concentration of Ca^{2+} was calculated for each mineral (from equation C2) and compared with the Ca^{2+} concentration determined experimentally.

Among these minerals, the Ca^{2+} concentration calculated for monetite (CaHPO_4) and brushite ($\text{CaHPO}_4 \cdot 2\text{H}_2\text{O}$) were the closest match with the experimental value (standard deviations of the calculated Ca^{2+} from the measured Ca^{2+} range from 0.004-0.370 and 0.201-1.38 for CaHPO_4 and $\text{CaHPO}_4 \cdot 2\text{H}_2\text{O}$, respectively) (Fig C.2). Ca^{2+} concentrations calculated from hydroxyapatite,

octacalcium phosphate and β -tricalcium phosphate were 1-4 order of magnitude lower than the measured concentration.

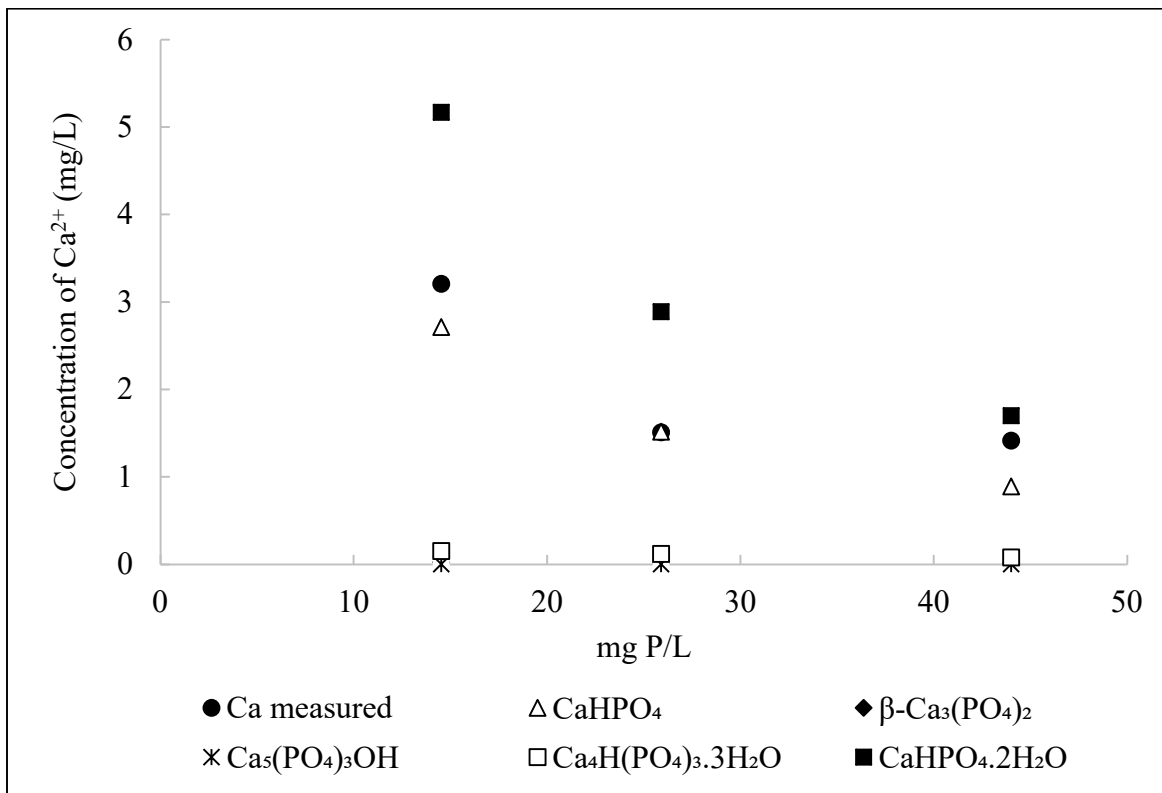


Fig. C.2. Concentrations of Ca^{2+} measured experimentally and theoretically from the solubility products of: brushite ($\text{CaHPO}_4 \cdot 2\text{H}_2\text{O}$), monetite (CaHPO_4), octacalcium phosphate ($\text{Ca}_4\text{H}(\text{PO}_4)_3 \cdot 3\text{H}_2\text{O}$), β -tricalcium phosphate ($\beta\text{-Ca}_3(\text{PO}_4)_2$) and hydroxyapatite ($\text{Ca}_5(\text{PO}_4)_3\text{OH}$) in phosphate solutions of deionized water at pH 10. Symbols for $\beta\text{-Ca}_3(\text{PO}_4)_2$ are below the symbols of $\text{Ca}_4\text{H}(\text{PO}_4)_3 \cdot 3\text{H}_2\text{O}$.

Appendix D: Cost analysis

This appendix includes cost calculation for production of one ton (metric ton) calcium silicate hydrate from rice husk. Later the costs of one ton phosphorus from calcium silicate hydrate and a commercial fertilizer-diammonium phosphate (DAP) were compared.

D.1 Production cost of one ton calcium silicate hydrate

The production cost for calcium silicate hydrate was computed based on raw material, chemicals and energy cost excluding the infrastructure cost for kiln, grinders, sieves, and wash basins. Prices of nitric acid and sodium hydroxide were taken from Echemi.com (2020) and the price for calcium nitrate tetrahydrate was taken from Alibaba.com (2020).

Price of rice husk was taken from national weekly rice summary, USDA Market news service (www.ams.usda.gov/mnreports/lr_gr410.txt, accessed on 6/12/20), assuming harvesting and labor cost were included in it. The price of rice hulls varied from \$5-15 per short ton, so an average price of \$10 per short ton was chosen. The price of rice hulls was converted to \$11/metric ton using the following conversion of unit: 1 short ton = 0.907185 metric ton.

To produce rice husk ash a large-scale pyrolysis kiln was considered, which is powered by natural gas and operated as a continuous process in a manner similar to industry prototypes under slow pyrolysis condition (Roberts et al., 2010). Volume of natural gas required for initial start-up of the kiln was assumed to be 1.67 m³/ton of feedstock, which was taken from the reported value of energy input to a pyrolysis/gasification plant to treat one ton of paint waste (Saft, 2007).

According to the experimental procedure, 5.19 g calcium silicate hydrate was produced from 3.0 g of rice husk. So, amount of rice husk required to produce 1 ton calcium silicate hydrate is,

$$\frac{3.0 \text{ g rice husk}}{5.19 \text{ g calcium silicate hydrate}} \times \left(\frac{1,000 \text{ g calcium silicate hydrate}}{1.0 \text{ kg calcium silicate hydrate}} \right) \times \left(\frac{1,000 \text{ kg calcium silicate hydrate}}{1.0 \text{ ton calcium silicate hydrate}} \right) = 580,000 \text{ g} = 0.58 \text{ ton.}$$

To wash 30 g of rice husk, 750 mL of 1 M HNO₃ solution was required, which can be reused 10 times. So, the volume of 1 M HNO₃ required to wash 0.58 ton rice husk is,

$$\left(\frac{750 \text{ mL 1 M HNO}_3}{30 \text{ g rice husk}} \times \frac{1,000,000 \text{ g rice husk}}{1.0 \text{ ton rice husk}} \times 0.58 \text{ ton rice husk} \right) \times \frac{1}{10} = 1,450,000 \text{ mL} = 1,450 \text{ L.}$$

The molarity of industrial grade 70% HNO₃ is, $\frac{70 \text{ g conc HNO}_3}{100 \text{ g of HNO}_3} \times \frac{1.41 \text{ g conc HNO}_3}{\text{mL of conc HNO}_3} \times$

$$\frac{1,000 \text{ mL of conc HNO}_3}{1.0 \text{ L of HNO}_3} \times \frac{1.0 \text{ mol}}{63 \text{ g HNO}_3} = 16 \text{ M (density of 70\% HNO}_3 \text{ is 1.41 g/mL).}$$

To prepare 1,450 L of 1 M HNO₃, the volume of 70% HNO₃ required is, $\frac{1,450 \text{ L} \times 1.0 \text{ M}}{16 \text{ M}} = 91 \text{ L.}$

So, the mass of 70% HNO₃ required to wash 0.58 ton rice husk is,

$$91 \text{ L} \times \frac{1.41 \text{ g}}{1.0 \text{ mL of HNO}_3} \times \frac{1,000 \text{ mL of conc HNO}_3}{1.0 \text{ L of HNO}_3} = 130,000 \text{ g} = 0.13 \text{ ton.}$$

To get 5.19 g calcium silicate hydrate, 3.0 g rice husk ash was dissolved in 300 mL of 0.164 M of NaOH. Also, to raise the pH of Ca(NO₃)₂ solution from 6.7 to 11.2, 1.5 mL of 1.0 M NaOH was used. So, total mass of NaOH to produce 5.19 g calcium silicate hydrate is,

$$\left(0.164 \text{ M} \times 300 \text{ mL} \times \frac{1.0 \text{ L}}{1,000 \text{ mL}} \times \frac{40 \text{ g}}{\text{L}} \right) + \left(1.0 \text{ M} \times 1.5 \text{ mL} \times \frac{1.0 \text{ L}}{1,000 \text{ mL}} \times \frac{40 \text{ g}}{\text{L}} \right) = 2.03 \text{ g.}$$

Mass of NaOH to produce 1.0 ton calcium silicate hydrate is,

$$\frac{2.03 \text{ g NaOH}}{5.19 \text{ g calcium silicate hydrate}} \times \left(\frac{1,000 \text{ g calcium silicate hydrate}}{1.0 \text{ kg calcium silicate hydrate}} \right) \times \left(\frac{1,000 \text{ kg calcium silicate hydrate}}{1.0 \text{ ton calcium silicate hydrate}} \right) = 390,000 \text{ g} = 0.39 \text{ ton.}$$

The dissolved silica was added to 300 mL of 0.158 M Ca(NO₃)₂·4H₂O to yield 5.19 g calcium silicate hydrate. So, mass of Ca(NO₃)₂·4H₂O required to prepare 5.19 g calcium silicate

hydrate is, $\left(0.158 \text{ M} \times 300 \text{ mL} \times \frac{1.0 \text{ L}}{1,000 \text{ mL}} \times \frac{236.15 \text{ g}}{\text{L}} \right) = 11.19 \text{ g.}$

Mass of $\text{Ca}(\text{NO}_3)_2 \cdot 4\text{H}_2\text{O}$ to produce 1.0 ton calcium silicate hydrate is,

$$\frac{11.19 \text{ g Ca}(\text{NO}_3)_2 \cdot 4\text{H}_2\text{O}}{5.19 \text{ g calcium silicate hydrate}} \times \left(\frac{1,000 \text{ g calcium silicate hydrate}}{1.0 \text{ kg calcium silicate hydrate}} \right) \times \left(\frac{1,000 \text{ kg calcium silicate hydrate}}{1.0 \text{ ton calcium silicate hydrate}} \right) = 2,200,000 \text{ g} = 2.2$$

ton.

The costs of raw material, chemicals, and fuel for production of one ton calcium silicate hydrate is summarized in Table D.1.

Table D.1 Summary of costs for production of one ton calcium silicate hydrate.

Description	Unit	Quantity	Unit price (\$/unit)	Total price (\$)
Material cost				
Rice husk	ton	0.58	11	6.4
Nitric acid	ton	0.13	206	27
Sodium hydroxide	ton	0.39	425	170
Calcium nitrate	ton	2.2	120 ¹	260
Fuel cost for pyrolysis operation				
Natural gas	cubic meter	1.67	0.105 ²	0.175
			Total	\$ 464

¹ The price of one ton 70% nitric acid was chosen as the mean of a range of prices (\$90-150) from Echemi.com.

² The price of natural gas for industrial use was \$2.97/1000 cubic foot according to U.S. Energy Information Administration (April 2020) which was converted to \$0.105/cubic meter by dividing the amount by (1000*0.0283).

D.2 Cost comparison of one ton phosphorus from calcium silicate hydrate and DAP fertilizer

Costs of calcium silicate hydrate and diammonium phosphate (DAP) fertilizer that provide one ton phosphorus were compared. DAP ((NH₄)₂HPO₄) fertilizer is one of the most widely used phosphorus fertilizers in United States (USDA, 2019). Like the phosphorus laden calcium silicate hydrate, DAP is high in phosphorus content and dissolves quickly under soil condition to release plant available phosphorus.

The mass of calcium silicate hydrate required to provide one ton phosphorus was calculated assuming that all the phosphorus removed from wastewater will be available to plants. All phosphorus present in diammonium phosphate was also assumed to be 100% available to plants.

The maximum uptake achieved by calcium silicate hydrate with a dosage of 3.0 g/L was 22.78 mg P/g (0.02278 g P/g of calcium silicate hydrate) at pH 9 in deionized water. Assuming 100% of the recovered phosphorus will be available to plants, the amount of calcium silicate hydrate required to yield one ton phosphorus is,

$$= \left(\frac{1.0 \text{ g solid}}{22.78 \text{ mg P}} \right) \times \left(\frac{1,000 \text{ mg P}}{1.0 \text{ g P}} \right) \times \left(\frac{1,000 \text{ g P}}{1.0 \text{ kg P}} \right) \times \left(\frac{1,000 \text{ kg P}}{1.0 \text{ ton P}} \right) = 44,000,000 \text{ g} = 44 \text{ ton}.$$

When calcium silicate hydrate was applied at 2.0 g/L, the maximum uptake observed was 34.14 mg P/g (0.03414 g P/g of calcium silicate hydrate) at pH 9 in deionized water. According to this result, the amount of calcium silicate hydrate required to yield one ton phosphorus is,

$$\left(\frac{1.0 \text{ g solid}}{34.14 \text{ mg P}} \right) \times \left(\frac{1,000 \text{ mg P}}{1.0 \text{ g P}} \right) \times \left(\frac{1,000 \text{ g P}}{1.0 \text{ kg P}} \right) \times \left(\frac{1,000 \text{ kg P}}{1.0 \text{ ton P}} \right) = 29,000,000 \text{ g} = 29 \text{ ton}.$$

Assuming all phosphorus in DAP (molecular weight = 132.06 g) is available to plants, the amount of DAP required to yield one ton phosphorus is,

$$\left(\frac{132.06 \text{ g DAP}}{30.97 \text{ g P}} \right) \times \left(\frac{1,000 \text{ g}}{1.0 \text{ kg}} \right) \times \left(\frac{1,000 \text{ kg}}{1.0 \text{ ton}} \right) = 43,000,000 \text{ g} = 4.3 \text{ ton}.$$

The comparison of prices of one ton phosphorus from calcium silicate hydrate and DAP fertilizer is summarized in Table D.2.

Table D.2 Comparison of prices for one ton phosphorus from calcium silicate hydrate and DAP fertilizer.

Material	Density of Phosphorus (g P/g of material)	Amount of material required to provide one ton phosphorus (ton)	Cost of material (\$/ton)	Cost to provide one ton phosphorus (1000 of \$)
Calcium silicate hydrate	0.023-0.034 ¹	29-44	464	14-20
DAP fertilizer	0.235	4.3	410 ²	1.8

¹ These values reflect phosphorus recovered by 2 and 3 g/L concentrations of calcium silicate hydrate.

² Cost of DAP was taken from the Bi-weekly Illinois Production Cost Report, USDA-Illinois department of Agricultural Market News Service, Springfield, IL, https://www.ams.usda.gov/mnreports/gx_gr210.txt, accessed in June 2020.

D.3 Cost improvement by using lime to synthesize calcium silicate hydrate

From Table D.1 it is evident that the most expensive component of the production cost of calcium silicate hydrate is chemical cost for calcium nitrate and sodium hydroxide. To avoid this, comparatively cheaper chemicals, such as lime (CaO) can be used to synthesize calcium silicate hydrate, as it can serve both a base and calcium source (James and Rao, 1985).

So, next the price of calcium silicate hydrate prepared by using CaO was estimated. To produce 5.19 g calcium silicate hydrate, the dissolved silica from rice husk ash was added to 300 mL of 0.158 M Ca(NO₃)₂·4H₂O. Assuming lime releases similar amount of Ca²⁺ as Ca(NO₃)₂

under the synthesis conditions, the mass of CaO necessary to produce 5.19 g calcium silicate hydrate is, $\left(0.158 \text{ M} \times 300 \text{ mL} \times \frac{1.0 \text{ L}}{1,000 \text{ mL}} \times \frac{56.08 \text{ g}}{\text{L}}\right) = 2.7 \text{ g}$.

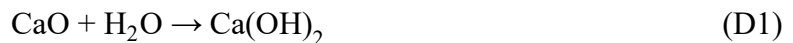
Mass of CaO required to produce 1 ton calcium silicate hydrate is, $\frac{2.7 \text{ g CaO}}{5.19 \text{ g calcium silicate hydrate}} \times \left(\frac{1,000 \text{ g calcium silicate hydrate}}{1.0 \text{ kg calcium silicate hydrate}}\right) \times \left(\frac{1,000 \text{ kg calcium silicate hydrate}}{1.0 \text{ ton calcium silicate hydrate}}\right) = 520,000 \text{ g} = 0.52$ ton.

Table D.3 Revised cost for production of one ton calcium silicate hydrate synthesized from lime instead of NaOH and $\text{Ca}(\text{NO}_3)_2 \cdot 4\text{H}_2\text{O}$.

Description	Unit	Quantity	Unit price (\$/unit)	Total price (\$)
Material cost				
Rice husk	ton	0.58	11	6.4
Nitric acid	ton	0.13	206	27
Lime	ton	0.52	80 ¹	42
Fuel cost for pyrolysis operation				
Natural gas	cubic meter	1.67	0.105	0.175
			Total	\$ 76

¹ Price of one ton lime was taken as the mean of a range of prices (\$60-100) from Alibaba.com (2020).

The lime would react with water according to the following reaction:



This would yield a OH^- concentration of $0.158 \times 2 = 0.316 \text{ M}$, which is 1.93 times higher than the concentration of sodium hydroxide needed to produce calcium silicate hydrate. So, it is safe to

assume that using lime will eliminate the requirement of NaOH. Using lime would reduce the cost of calcium silicate hydrate to \$76/ ton which is 84% lower than the previous cost. The cost of one ton phosphorus from calcium silicate hydrate synthesized from lime was estimated to be \$2200-3300 which is quite comparable to the cost of phosphorus from DAP fertilizer (\$1800) (Table D.4), making it a viable alternative to commercially available phosphorus fertilizers.

Table D.4 Revised comparison of the prices for one ton phosphorus from calcium silicate hydrate (synthesized from lime) and from DAP fertilizer.

Material	Density of Phosphorus (g P/g of material)	Amount of material required to provide one ton phosphorus (ton)	Cost of material (\$/ton)	Cost to provide one ton phosphorus (1000 of \$)
Calcium silicate hydrate	0.023-0.034	29-44	76	2.2-3.3
DAP fertilizer	0.235	4.3	410	1.8

References

- Abedin, M. J., Cresser, M. S., Meharg, A. A., Feldmann, J., & Cotter-Howells, J. (2002). Arsenic accumulation and metabolism in rice (*Oryza sativa* L.). *Environmental science & technology*, 36(5), 962-968.
- Adeleke, R., Nwangburuka, C., & Oboirien, B. (2017). Origins, roles and fate of organic acids in soils: A review. *South African Journal of Botany*, 108, 393-406.
- Aguilar, M. I., Saez, J., Llorens, M., Soler, A., & Ortuno, J. F. (2002). Nutrient removal and sludge production in the coagulation–flocculation process. *Water research*, 36(11), 2910-2919.
- Alfa, M. I., Adie, D. B., Igboro, S. B., Oranusi, U. S., Dahunsi, S. O., & Akali, D. M. (2014). Assessment of biofertilizer quality and health implications of anaerobic digestion effluent of cow dung and chicken droppings. *Renewable Energy*, 63, 681-686.
- Aprianti, E., Shafiqh, P., Bahri, S., & Farahani, J. N. (2015). Supplementary cementitious materials origin from agricultural wastes—A review. *Construction and Building Materials*, 74, 176-187.
- Ayral, A., Julbe, A., Rouessac, V., Roualdes, S., & Durand, J. (2008). Microporous silica membrane: basic principles and recent advances. *Membrane science and technology*, 13, 33-79.
- Balakrishnan, M., Batra, V.S., Hargreaves, J.S.J. and Pulford, I.D. (2011) Waste materials - catalytic opportunities: an overview of the application of large scale waste materials as resources for catalytic applications. *Green Chemistry* 13(1), 16-24.
- Berg, U., Donnert, D., Ehbrecht, A., Bumiller, W., Kusche, I., Weidler, P. G., & Nüesch, R. (2005). “Active filtration” for the elimination and recovery of phosphorus from wastewater. *Colloids and Surfaces A: Physicochemical and Engineering Aspects*, 265(1-3), 141-148.

Banu, R. J., Do, K. U., & Yeom, I. T. (2008). Phosphorus removal in low alkalinity secondary effluent using alum. *International Journal of Environmental Science & Technology*, 5(1), 93-98.

Barber, S. A. (1984). *Soil nutrient bioavailability* (John Wiley & Sons: New York). Soil nutrient bioavailability. John Wiley & Sons, New York.

Bray, R. H., & Kurtz, L. T. (1945). Determination of total, organic, and available forms of phosphorus in soils. *Soil science*, 59(1), 39-46.

Burns, R. T., & Moody, L. B. (2002). Phosphorus recovery from animal manures using optimized struvite precipitation. *Proceedings of Coagulants and Flocculants: Global Market and Technical Opportunities for Water Treatment Chemicals*, May.

Cabeza, R., B. Steingrobe, W. Romer, and N. Claassen. 2011. Effectiveness of recycled P products as P fertilizers, as evaluated in pot experiments. *Nutrient Cycling in Agroecosystems* 91: 173–184.

Caravelli, A. H., Contreras, E. M., & Zaritzky, N. E. (2010). Phosphorous removal in batch systems using ferric chloride in the presence of activated sludges. *Journal of hazardous materials*, 177(1-3), 199-208.

Chalmers, R. A., & Sinclair, A. G. (1966). Analytical applications of β -heteropoly acids: This influence of complexing agents on selective formation. *Analytica Chimica Acta*, 34, 412-418.

Chandrasekhar, S., Satyanarayana, K.G., Pramada, P.N., Raghavan, P. and Gupta, P.N. (2003) Review Processing, properties and applications of reactive silica from rice husk—an overview. *Journal of Materials Science* 38, 3159–3168.

Chen, J.J., Thomas, J.J., Taylor, H.F.W. and Jennings, H.M. (2004) Solubility and structure of calcium silicate hydrate. *Cement and Concrete Research* 34(9), 1499-1519.

Chow, L. C. (1991). Development of self-setting calcium phosphate cements. *Journal of the Ceramic society of Japan*, 99(1154), 954-964.

Chuang, S. H., Chang, W. C., Chang, T. C., & You, S. J. (2006). Improving the removal of anions by coagulation and dissolved air flotation in wastewater reclamation. *Environmental technology*, 27(5), 493-500.

Cong, X., & Kirkpatrick, R. J. (1996). ²⁹Si MAS NMR study of the structure of calcium silicate hydrate. *Advanced Cement Based Materials*, 3(3-4), 144-156.

Cordell, D., Drangert, J.O. and White, S. (2009) The story of phosphorus: Global food security and food for thought. *Global Environmental Change-Human and Policy Dimensions* 19(2), 292-305.

Correll, D. L. (1998). The role of phosphorus in the eutrophication of receiving waters: A review. *Journal of environmental quality*, 27(2), 261-266.

Davis, H. F., & Harshman, J. P. (1991). U.S. Patent No. 5,013,442. Washington, DC: U.S. Patent and Trademark Office.

Desmidt, E., Ghyselbrecht, K., Zhang, Y., Pinoy, L., Van der Bruggen, B., Verstraete, W., ... & Meesschaert, B. (2015). Global phosphorus scarcity and full-scale P-recovery techniques: a review. *Critical Reviews in Environmental Science and Technology*, 45(4), 336-384.

Dickman, S. R., & Bray, R. H. (1941). Replacement of adsorbed phosphate from kaolinite by fluoride. *Soil Science*, 52(4), 263-274.

Dorozhkin, S. V. (2007). Calcium orthophosphates. *Journal of materials science*, 42(4), 1061-1095.

Drouet, C. (2013). Apatite formation: why it may not work as planned, and how to conclusively identify apatite compounds. *BioMed research international*, 2013.

Eanes, E. D., Termine, J. D., & Nysten, M. U. (1973). An electron microscopic study of the formation of amorphous calcium phosphate and its transformation to crystalline apatite. *Calcified tissue research*, 12(1), 143-158.

Edixhoven, J. D., Gupta, J., & Savenije, H. H. G. (2014). Recent revisions of phosphate rock reserves and resources: a critique. *Earth System Dynamics*, 5(2), 491-507.

El Damatty, A. A., & Hussain, I. (2009). An economical solution for the environmental problem resulting from the disposal of rice straw. In *Appropriate Technologies for Environmental Protection in the Developing World* (pp. 15-23). Springer, Dordrecht.

Fang, D., Huang, L., Fang, Z., Shen, Q., Li, Y., Xu, X. and Ji, F. (2018) Evaluation of porous calcium silicate hydrate derived from carbide slag for removing phosphate from wastewater. *Chemical Engineering Journal*, 354, 1-11.

Ferguson, J. F., & McCarty, P. L. (1971). Effects of carbonate and magnesium on calcium phosphate precipitation. *Environmental Science & Technology*, 5(6), 534-540.

Galhardo, C. X., & Masini, J. C. (2000). Spectrophotometric determination of phosphate and silicate by sequential injection using molybdenum blue chemistry. *Analytica Chimica Acta*, 417(2), 191-200.

Georgantas, D. A., & Grigoropoulou, H. P. (2007). Orthophosphate and metaphosphate ion removal from aqueous solution using alum and aluminum hydroxide. *Journal of Colloid and Interface Science*, 315(1), 70-79.

Giesen, A. (1999). Crystallisation process enables environmental friendly phosphate removal at low costs. *Environmental Technology*, 20(7), 769-775.

Glushankova, I., Ketov, A., Krasnovskikh, M., Rudakova, L., & Vaisman, I. (2018). Rice hulls as a renewable complex material resource. *Resources*, 7(2), 31.

Guan, W., Ji, F.Y., Chen, Q.K., Yan, P. and Zhou, W.W. (2013) Influence of Hydrothermal Temperature on Phosphorus Recovery Efficiency of Porous Calcium Silicate Hydrate. *Journal of Nanomaterials* 2013, 6 pages.

Gungor, K. and Karthikeyan, K.G. (2008) Phosphorus forms and extractability in dairy manure: A case study for Wisconsin on-farm anaerobic digesters. *Bioresource Technology* 99(2), 425-436.

Houston, J. R., Maxwell, R. S., & Carroll, S. A. (2009). Transformation of meta-stable calcium silicate hydrates to tobermorite: reaction kinetics and molecular structure from XRD and NMR spectroscopy. *Geochemical Transactions*, 10(1), 1-14.

Huchzermeier, M.P. and Tao, W.D. (2012) Overcoming Challenges to Struvite Recovery from Anaerobically Digested Dairy Manure. *Water Environment Research* 84(1), 34-41.

IFDC (2010) Sufficient phosphate rock resources Available for years. International Fertilizer Development Center, Muscle Shoals, AL 35662, USA. Report 35: 1.

Islam, S., Rahman, M. M., Islam, M. R., & Naidu, R. (2016). Arsenic accumulation in rice: consequences of rice genotypes and management practices to reduce human health risk. *Environment international*, 96, 139-155.

James, J., & Rao, M. S. (1986). Reaction product of lime and silica from rice husk ash. *Cement and Concrete Research*, 16(1), 67-73.

Jensen, J. N. (2003). *A problem-solving approach to aquatic chemistry*. New York: Wiley.

Jiang, D., Amano, Y., & Machida, M. (2017). Removal and recovery of phosphate from water by calcium-silicate composites-novel adsorbents made from waste glass and shells. *Environmental Science and Pollution Research*, 24(9), 8210-8218.

Johnston, A. E., & Richards, I. R. (2003). Effectiveness of different precipitated phosphates as phosphorus sources for plants. *Soil use and management*, 19(1), 45-49.

Jordaan, E. M., Ackerman, J., & Cicek, N. (2010). Phosphorus removal from anaerobically digested swine wastewater through struvite precipitation. *Water Science and Technology*, 61(12), 3228-3234.

Karimi, K., Emtiazi, G., & Taherzadeh, M. J. (2006). Ethanol production from dilute-acid pretreated rice straw by simultaneous saccharification and fermentation with *Mucor indicus*, *Rhizopus oryzae*, and *Saccharomyces cerevisiae*. *Enzyme and microbial technology*, 40(1), 138-144.

Koenig, L. E., Baumann, A. J., & McDowell, W. H. (2014). Improving automated phosphorus measurements in freshwater: an analytical approach to eliminating silica interference. *Limnology and Oceanography: Methods*, 12(4), 223-231.

Kumar, A., Mohanta, K., Kumar, D. and Parkash, O. (2012), Properties and Industrial Applications of Rice husk: A review, *International Journal of Emerging Technology and Advanced Engineering*, Volume 2, Issue 10, 2250 2459.

Kumar, R., & Pal, P. (2015). Assessing the feasibility of N and P recovery by struvite precipitation from nutrient-rich wastewater: a review. *Environmental Science and Pollution Research*, 22(22), 17453-17464.

Kuwahara, Y., Tamagawa, S., Fujitani, T. and Yamashita, H. (2013) A novel conversion process for waste slag: synthesis of calcium silicate hydrate from blast furnace slag and its application as a versatile adsorbent for water purification. *Journal of Materials Chemistry A* 1(24), 7199-7210.

Le Corre, K. S., Valsami-Jones, E., Hobbs, P., & Parsons, S. A. (2009). Phosphorus recovery from wastewater by struvite crystallization: A review. *Critical Reviews in Environmental Science and Technology*, 39(6), 433-477.

Li, Y., Liu, W., Xing, F., Wang, S., Tang, L., Lin, S., & Dong, Z. (2020). Carbonation of the synthetic calcium silicate hydrate (CSH) under different concentrations of CO₂: Chemical phases analysis and kinetics. *Journal of CO₂ Utilization*, 35, 303-313.

Mehlich, A. (1984). Mehlich 3 soil test extractant: A modification of Mehlich 2 extractant. *Communications in soil science and plant analysis*, 15(12), 1409-1416.

Memon, S. A., Khan, S., Wahid, I., Shestakova, Y., & Ashraf, M. (2020). Evaluating the Effect of Calcination and Grinding of Corn Stalk Ash on Pozzolanic Potential for Sustainable Cement-Based Materials. *Advances in Materials Science and Engineering*, 2020.

Mupa, M., Hungwe, C. B., Witzleben, S., Mahamadi, C., & Muchanyereyi, N. (2015). Extraction of silica gel from Sorghum bicolour (L.) moench bagasse ash. *African Journal of Pure and Applied Chemistry*, 9 (2), 12-17.

Nasrazadani, S., & Hassani, S. (2016). Modern analytical techniques in failure analysis of aerospace, chemical, and oil and gas industries. In *Handbook of Materials Failure Analysis with Case Studies from the Oil and Gas Industry* (pp. 39-54). Butterworth-Heinemann.

Nonat, A. (2004) The structure and stoichiometry of C-S-H. *Cement and Concrete Research* 34(9), 1521-1528.

Olsen, S. R. (1954). Estimation of available phosphorus in soils by extraction with sodium bicarbonate (No. 939). US Department of Agriculture.

Okano, K., Uemoto, M., Kagami, J., Miura, K., Aketo, T., Toda, M., Honda, K. & Ohtake, H. (2013). Novel technique for phosphorus recovery from aqueous solutions using amorphous calcium silicate hydrates (A-CSHs). *Water Research*, 47(7), 2251-2259.

Okano, K., Miyamaru, S., Kitao, A., Takano, H., Aketo, T., Toda, M., Honda, K. & Ohtake, H. (2015). Amorphous calcium silicate hydrates and their possible mechanism for recovering phosphate from wastewater. *Separation and Purification Technology*, 144, 63-69.

Okano, K., Yamamoto, Y., Takano, H., Aketo, T., Honda, K., & Ohtake, H. (2016). A simple technology for phosphorus recovery using acid-treated concrete sludge. *Separation and Purification Technology*, 165, 173-178.

Oladoja, N. A., Ololade, I. A., Adesina, A. O., Adelagun, R. O. A. and Sani, Y.M. (2013). Appraisal of gastropod shell as calcium ion source for phosphate removal and recovery in calcium phosphate minerals crystallization procedure. *Chemical Engineering Research & Design*, 91(5), 810–818.

Panda, S. K., Baluska, F., & Matsumoto, H. (2009). Aluminium stress signaling in plants. *Plant Signal Behav* 4 (7): 592–597.

Parsons, S. A., & Smith, J. A. (2008). Phosphorus removal and recovery from municipal wastewaters. *Elements*, 4(2), 109-112.

Peng, L., Dai, H., Wu, Y., Peng, Y., & Lu, X. (2018). A comprehensive review of the available media and approaches for phosphorus recovery from wastewater. *Water, Air, & Soil Pollution*, 229(4), 115.

Permatasari, N., Sucahya, T. N., & Nandiyanto, A. B. D. (2016). Agricultural wastes as a source of silica material. *Indonesian journal of science and technology*, 1(1), 82-106.

Pierzynski, G. M. (2000). Methods of phosphorus analysis for soils, sediments, residuals, and waters. Southern Cooperative Series, Bulletin No. 396, SERA-IEG-17.

Plaza C, Sanz R, Clemente C, Fernández JM, González R, Polo A, Colmenarejo MF (2007) Greenhouse evaluation of struvite and sludges from municipal wastewater treatment works as phosphorus sources for plants. *J Agric Food Chem* 55:8206–8212.

Perera, P., Han, Z. Y., Chen, Y. X., & Wu, W. X. (2007). Recovery of nitrogen and phosphorous as struvite from swine waste biogas digester effluent. *Biomed Environ Sci*, 20(5), 343-350.

Rahman, M. A., Hasegawa, H., Rahman, M. M., Rahman, M. A., & Miah, M. A. M. (2007). Accumulation of arsenic in tissues of rice plant (*Oryza sativa* L.) and its distribution in fractions of rice grain. *Chemosphere*, 69(6), 942-948.

Resende, J. A., Silva, V. L., de Oliveira, T. L. R., de Oliveira Fortunato, S., da Costa Carneiro, J., Otenio, M. H., & Diniz, C. G. (2014). Prevalence and persistence of potentially pathogenic and antibiotic resistant bacteria during anaerobic digestion treatment of cattle manure. *Bioresource technology*, 153, 284-291.

- Roberts, K. G., Gloy, B. A., Joseph, S., Scott, N. R., & Lehmann, J. (2010). Life cycle assessment of biochar systems: estimating the energetic, economic, and climate change potential. *Environmental science & technology*, 44(2), 827-833.
- Roselló, J., Soriano, L., Santamarina, M. P., Akasaki, J. L., Melges, J. L. P., & Payá, J. (2015). Microscopy characterization of silica-rich agrowastes to be used in cement binders: bamboo and sugarcane leaves. *Microscopy and Microanalysis*, 1314-1326.
- Rittmann, B.E., Mayer, B., Westerhoff, P. and Edwards, M. (2011) Capturing the lost phosphorus. *Chemosphere* 84(6), 846-853.
- Saft, R. J. (2007). Life cycle assessment of a pyrolysis/gasification plant for hazardous paint waste. *The International Journal of Life Cycle Assessment*, 12(4), 230.
- Sahrawat, K. Á. (2005). Iron toxicity in wetland rice and the role of other nutrients. *Journal of plant nutrition*, 27(8), 1471-1504.
- Sanchez, E., Borja, R., Weiland, P., Travieso, L. and Martin, A. (2000) Effect of temperature and pH on the kinetics of methane production, organic nitrogen and phosphorus removal in the batch anaerobic digestion process of cattle manure. *Bioprocess Engineering* 22(3), 247-252.
- Schröder J. J., Cordell, D., Smit, A. L., and Rosemarin, A.: Sustainable Use of Phosphorus, EU tender EN V. B.1/ETU/2009/0025, Plant research International, Business Unit Agrosystems, Wageningen UR, the Netherlands, 2010.
- Song, Y., Hahn, H. H., & Hoffmann, E. (2002). The effect of carbonate on the precipitation of calcium phosphate. *Environmental technology*, 23(2), 207-215.

Terzioğlu, P., Yucel, S., Rabagah, T. M., & Özçimen, D. (2013). Characterization of wheat hull and wheat hull ash as a potential source of SiO₂. *BioResources*, 8(3), 4406-4420.

USDA (2019) Fertilizer use and price. Economic Research Service, <https://www.ers.usda.gov/data-products/fertilizer-use-and-price/>, Accessed 8/15/20.

Vaibhav, V., Vijayalakshmi, U. and Roopan, S.M. (2015) Agricultural waste as a source for the production of silica nanoparticles. *Spectrochimica Acta Part a-Molecular and Biomolecular Spectroscopy* 139, 515-520.

Vanotti, M.B., Szogi, A.A. and Hunt, P.G. (2003) Extraction of soluble phosphorus from swine wastewater. *Transactions of the Asae* 46(6), 1665-1674.

Wan, X.H., Chang, C.K., Mao, D.L., Jiang, L. and Li, M. (2005) Preparation and in vitro bioactivities of calcium silicate nanophase materials. *Materials Science & Engineering C-Biomimetic and Supramolecular Systems* 25(4), 455-461.

Yao, X., Xu, K., & Liang, Y. (2016). Analytical Pyrolysis Study of Peanut Shells using TG-MS Technique and Characterization for the Waste Peanut Shell Ash. *Journal of Residuals Science & Technology*, 13(4).

Zhou, Y., Selvam, A., & Wong, J. W. (2014). Evaluation of humic substances during co-composting of food waste, sawdust and Chinese medicinal herbal residues. *Bioresource Technology*, 168, 229-234.